This is a repository copy of *Finite element analysis of polyethylene wear in total hip replacement: A literature review*.

White Rose Research Online URL for this paper:
http://eprints.whiterose.ac.uk/160383/

Version: Accepted Version

Article:

Finite Element Analysis of Polyethylene Wear in Total Hip Replacement: A Literature Review

Lin Wang[1, 2*], Graham Isaac[2], Ruth Wilcox[2], Alison Jones[2], Jonathan Thompson[1, 2]

*Corresponding author. Tel: +44 113 387 7800; Fax. +44 113 387 7893; E-mail: lwang75@its.jnj.com.

[1] Hip Development, Worldwide Research & Development, DePuy Synthes Joint Reconstruction, Leeds, LS11 8DT, UK

[2] Institute of Medical and Biological Engineering, School of Mechanical Engineering, University of Leeds, Leeds, LS2 9JT, UK

Abstract:

Evaluation and prediction of wear play a key role in product design and material selection of total hip replacements, because wear debris is one of the main causes of loosening and failure. Multifactorial clinical or laboratory studies are high cost and require unfeasible timeframes for implant development. Simulation using finite element (FE) methods is an efficient and inexpensive alternative to predict wear and pre-screen various parameters. This paper presents a comprehensive literature review of the state-of-the-art FE modelling techniques that have been applied to evaluate wear in polyethylene hip replacement components. A number of knowledge gaps are identified including the need to develop appropriate wear coefficients and the analysis of daily living activities.

Keywords: Artificial Hip Joint; Biotribology; Contact Modelling; Wear Modelling; Wear Mechanics.

Abbreviations:

UHMWPE: Ultra-High-Molecular-Weight Polyethylene

FEA: Finite Element Analysis

THR: Total Hip Replacement

MoP: Metal-on-Polyethylene

PoD: Pin-on-Disk

RSA: Radiostereometric Analysis

3D: 3-Dimensional

2D: 2-Dimensional

MoM: Metal-on-Metal

CoCr: Cobalt-Chrome alloy

CSR: Cross Shear Ratio

1

DLC: Diamond-Like Carbon

SS: Stainless Steel

PMO: Principal Molecular Orientation

Mc: million cycles

CMM: Coordinate Measuring Machine

1. Introduction

The hip joint is a type of diarthrodial joint, also known as a ball-in-socket joint: the head of the femur is the ball and the acetabulum constitutes the socket. In a normal hip, a smooth layer of cartilage separates the ball and the socket, allowing the ball to glide easily within the socket, cushioning the joint [1]. However, the hip may wear out, usually as a cause of degenerative disease such as osteoarthritis, at different stages of a person's life. Hip joint implants are designed to replace biological materials which are damaged, aiming to reduce joint pain, enhance joint function and improve quality of life for patients. Total Hip Replacement (THR) is a successful and cost effective solution for hip joint diseases and also one of the most common surgeries performed in the world. The number of people undergoing this operation is set to rise, resulting from an ageing population. At the same time, increasing numbers of younger and more active patients are undergoing THR surgery, placing additional demands on the device performance.

Polyethylene total hip joints, which consist of a metallic/ceramic femoral head articulating against an Ultra-High-Molecular-Weight Polyethylene (UHMWPE) liner as shown in Figure 1, are clinically the most widely implanted. Hip replacement may require revision (or replacement) for a variety of reasons, both biological and mechanical. The most common long term cause is "aseptic loosening" [2], which has been associated with a number of underlying factors [3], including the release of UHMWPE wear debris. Over the past decade, cross-linked UHMWPE biomaterials have been introduced to decrease surface wear. However cross-linking also reduces the mechanical properties [4] and although results to date are encouraging, these materials have not been commercialized long enough to clinically demonstrate they can improve the lifespan of THR [5]. Therefore, evaluation and prediction of UHMWPE wear play a key role in the product design and material selection of THR. The average wear rate of conventional and cross-linked UHMWPE in metal-on-polyethylene prostheses, both *In vivo* and *in vitro,* are listed in Table 1 [5, 6].

Figure 1 Polyethylene total hip joint. Image courtesy of DePuy Synthes, Leeds, UK

Table 1 *In vivo* and *in vitro* wear rate of MoP (Metal-on-Polyethylene) prostheses [5, 6]

There are generally three approaches when analysing the UHMWPE liner wear: laboratory experiment, clinical investigation and numerical analysis. Laboratory studies include Pin-on-Disk (PoD) and hip joint simulator testing. PoD testing is useful to characterise wear properties under various conditions, e.g. changes in pressure, cross shear or surface roughness. The hip joint simulator is a standardised method developed to replicate the motion and loading profile of a patient's hip joint, in a simulated *in vivo* environment, and as such has become an indispensable method to assess the wear performance of any new bearing design. However, it is very time consuming and expensive to run with a test of few million cycles taking months to complete. Moreover most simulators can only run under a set of standard conditions which simulate walking.

Clinical studies include the evaluation of retrieved implants, the assessment of penetration depth using measurements of femoral head migration rate on follow-up x-rays or radiostereometric analysis (RSA)[7]. However, wear takes place in three dimensions (3D), and it is difficult to obtain accurate results by 2D x-ray. Although RSA allows 3D measurement, it is quite expensive and intrusive. Most importantly, clinical studies are not under controlled conditions due to the variation in patient activity, lubrication, liner oxidation and roughness of the femoral head. Hence a wide range of wear rates are found clinically.

Recent developments in understanding of variable outcomes in hip replacement have led to increasing need for the development of wear simulation methods which address more complex surgical and patient scenarios (e.g. inclusion of stop-dwell-start motion [8, 9], obese patient profiles [10, 11], component separation [12, 13], and variation in component positioning [14-17]). Carrying out multi-factorial clinical and laboratory studies with material, design and manufacturing as well as surgical-patient parameters makes the cost and time for developing implants unrealistic. To address those challenges and limitations, long term wear has been predicted by more efficient and less expensive numerical approaches e.g. mathematical modelling and finite element analysis (FEA). Mathematical wear modelling employs many simplifications such as ideal rigid coupling [18] and Hertzian pressure distribution theory [19]; creep, friction and the geometrical evolution of wear are neglected [20]. Such modelling is rarely pursued and not the focus of this paper. Finite Element Analysis (FEA) of hip joint bearing wear, which was pioneered by Maxian et al [21-23] and adapted by a considerable number of researchers over the past two decades, allows more comprehensive algorithms to simulate the contact behavior, to gain understanding of the wear mechanics and provide initial screening of various parameters. More importantly, the numerical technique is also applicable to other types of joint replacements and has been employed on the wear prediction of knee [24-31], shoulder [32-36], ankle [37-39] and spine [40, 41]. Nevertheless, the accuracy of FEA prediction depends on inputs from

laboratory experiments and it is critical to validate the FEA model before it can provide guidance to testing and assist product development.

To the best of our knowledge, there has only been one review regarding FEA of wear at the articulating surface of THR [42], which was published in 2010. The aim of this paper was to deliver a comprehensive literature review of the state-of-the-art FEA modelling techniques and numerical wear mechanics analyses of UHMWPE liner wear, including discussion n of the limitations of current methodologies and identification of the knowledge gaps for future studies. Theoretical foundations of the finite element method are widely explained in textbooks [43, 44] and are not discussed here, but specific FEA techniques relevant to this review are summarised in the relevant sections. The review was conducted using ScienceDirect (https://www.sciencedirect.com/) and PubMed (https://www.ncbi.nlm.nih.gov/pubmed). Combinations of keywords comprising "total hip replacement", "hip joint" or "hip arthroplasty" along with "polyethylene wear" and "finite element analysis", "modelling" or "prediction" were used. Papers were included that were published in English between 1996 and 2016. The abstracts were then examined for relevance to the aim of this study, yielding a total of 28 publications. Section 2 and 3 of this paper detail the methodology of contact and wear modelling of the UHMWPE liner, respectively. Section 4 discusses the mechanics of wear and creep, and parametric studies are presented in Section 5. Finally, discussion and conclusion of this literature review are summarised in Section 6 and 7, respectively.

2. FEA Contact Modelling

Finite Element Analysis (FEA) is a numerical method seeking an approximated solution of a complex engineering problem which is difficult to obtain analytically or has no analytical solution. FEA has been used widely in the evaluation of orthopaedic devices since the 1970s. The rapid development of computational capability has enabled increasingly complex problems to be evaluated including the analysis of bone adaption, tissue differentiation, damage accumulation and wear [45].

The workflow of modelling UHMWPE liner contact and wear mechanics, which require inputs of geometry, material, loading and motion, as illustrated in Figure 2. At every time increment, the wear depth of each node on the bearing contact surface is calculated and the nodal position is updated accordingly. Then the updated geometry of the UHMWPE liner is used in the contact mechanics analysis, and subsequent wear prediction at the next time increment. This process repeats until the end of the pre-defined load cycle.

Figure 2 Workflow of FEA modelling of liner wear

2.1 Model Geometry

Most FEA wear models of THR have employed a 3D ball-in-socket assembly, as shown in Figure 3, and consist of three components: the femoral head, metal shell and liner. The supporting bone geometry has been found to have negligible effects on wear [46, 47]. In addition, to improve computing efficiency, the head and shell were generally assumed to be rigid bodies [48-50], because their stiffness is considerably higher than the deformable UHMWPE liner. Other FEA models have been simplified by eliminating the metal shell and applying constraints to the outer surface of the liner [51-53]. This simplification was justified by Barreto et al [47], because without the metal shell the volumetric wear rate was found to increase by less than 1%, compared to the FEA with the metal shell. Nevertheless, a limitation of this approach is that it is not able to analyse the press fit, locking mechanism and backside wear between the liner and shell.

Figure 3 An exploded view of the three components commonly modelled in FEA of UHMWPE liner wear

2.2 Mesh Configuration

There have been two commonly used mesh configurations for a liner FEA model. The "polar" design [21, 22], as shown in Figure 4(a), employs a circumferential sweep operation, using hexahedral elements for majority of the liner and wedge elements in the central region. Two possible shortcomings of this mesh configuration are: 1) mixing different type of element often results in irregular stress concentrations not related to the load applied [54] and 2) the small wedge elements could limit the time increment in an explicit FEA, hence increase the computational cost [55]. The "butterfly" design [50-54, 56-58], as shown in Figure 4(b), employs a radial sweep operation to ensure the accuracy and efficiency of wear modelling by preventing the use of wedge elements. Despite the fact that both configurations are widely used, there have been no direct comparisons made between them.

Figure 4 Two commonly used liner mesh configurations: (a) "polar" design, (b) "butterfly" design.

2.3 Material Model

In earlier FEA wear models, the UHMWPE liner was assumed as an isotropic and linear elastic material, i.e. using a pure elastic model [21-23, 46, 51, 52], with a Young's modulus of 1.4 GPa and a Poisson's ratio of 0.3 [59]. However, this assumption is no longer valid if the UHMWPE material

begins to exhibit plasticity due to severe load conditions. To take the nonlinear stress-strain behaviour of UHMWPE material into account, a simplified perfectly plastic model was introduced [54]. However, this model offers no further resistance to material deformation upon the yielding stress limit, as shown in Figure 5. More accurate strain hardening models have also been employed [49, 53, 60, 61], where the stress– strain relationship of UHMWPE is described by multi-linear data. Based on a compressive characterisation of UHMWPE at 37°C performed by Cripton [62], Matsoukas et al [53, 61] assumed a constant modulus of 110MPa beyond the yielding stress of 17MPa and they derived an equation to describe the stress (σ) – strain (ε) behaviour with 100 points up to yielding:

$$\sigma = 20.29(1 - e^{-32.485\varepsilon}) \tag{1}$$

Figure 5 Schematic stress-strain behaviour exhibited by different material models used to represent the UHMWPE liner

2.4 Loading & Boundary Conditions

The loads and motions applied to the FEA models have been generally obtained from gait studies of patients with instrumented THRs [63] or simplified conditions such as ISO 14242 [64] or hip simulator inputs [65]. Amongst various daily activities, normal walking has been extensively studied. Load inputs for the models were generally applied to the femoral head, consisting of either all the three force components [21-23, 48, 51, 54, 61, 66] or just the superior-inferior components [50, 53, 58, 65, 67]. Until now, no direct comparative study has been carried out between the 3D and 1D loading cases, which may be critical to understand the effects of the less dominant anterior-posterior and medial-lateral force components on UHMWPE liner wear. Rotations of the head have been applied as boundary conditions on the head [50] or on both the head and liner [53, 65], depending on the setup of the hip simulator being modelled. While some studies have used all three angular movements [48, 61, 68], only the flexion-extension angle profile was used by others [21-23, 50, 51, 58], which may consequently under-predict the wear compared to clinical data due to the cross shear effect of the other motions [54] and decrease in the sliding distance [57]. In almost all the models, the outer surfaces of the metal shells have been constrained, to prevent rigid body motion. To assist model convergence for static wear FEA, displacement control has been used to establish the initial contact, then changing to load control [23]. It is also worth noting that in early studies, the swing phase of the gait cycle was neglected for computational economy [21-23, 46, 51, 56, 57, 69]. However, this simplification may result in under-prediction of the wear, as relative motion between the head and liner during swing phase would still generate some wear, despite the fact that loading of the swing phase is much lower than it is in the stance phase.

2.5 Solution Method

Finite Element solution methods are generally divided into the implicit and the explicit methods [70]. The implicit FEA method iterates to find the approximate static equilibrium at the end of each load increment. For a nonlinear problem, the computation can be extremely expensive because the global stiffness matrix has to be assembled and inverted many times. Therefore, the implicit method is preferable to analyse static problems, where the load is time independent and inertial effects are negligible in contrast to dynamic problems. Until now, almost all the FEA modelling of contact and wear mechanics of UHMWPE hip joints have employed the implicit solution method. The explicit method determines a solution by advancing the kinematic state from one time increment to the next, without iteration. It is more robust and efficient for complicated problems, such as dynamic events, nonlinear behaviours, and complex contact conditions. However, in order to obtain accurate results from the explicit method, the time increment has to be extremely small to ensure that the acceleration through the time increment is nearly constant. Therefore an explicit analysis typically requires many thousands of increments. To date, explicit FEA studies have been utilised mainly on knee joint replacements to analyse the kinematics and contact mechanics during dynamic loading conditions [71-75] and the complex contact mechanics of the MoM hip joint under edge loading conditions [76]. Recently, it has been reported that the explicit FEA was able to accurately predict both the contact pressure and sliding distance of artificial hip and knee joints [77], when compared with the corresponding implicit FEA. However, no attempts have been made to explore the options of predicting UHMWPE liner wear by using explicit FEA and to benchmark its computational efficiency against implicit FEA.

2.6 Contact Treatment

To date, all UHMWPE liner wear FEA models simulated dry contact between articulating surfaces, where lubrication was neglected. For a classic three-component ball-in-socket model, there are two contact pairs: the head/liner articulating interface and the liner/shell interface. The head/liner interface is the main source of wear generation. Friction at this interface was neglected in the early studies [21-23]. This assumption, however, is unlikely to remain valid in the longer term, especially once wear occurs [54]. Although an experimental study has shown that friction between UHMWPE liner and CoCr head decreases as contact stress increases [78], the frictional coefficients have been simplified and assumed to be constant in the contact and subsequent wear FEA with slightly varying values (0.04 [53]; 0.06 [79]; 0.07 [47, 57]; 0.08 [61] and 0.083 [50]). Nevertheless, it is worth noting that the wear has been found to be insensitive to the frictional coefficient within this range [53, 54]. The liner/shell interface has been generally simplified as bonded contact [21-23, 46] or modelled as frictional contact with a coefficient of 0.083 in order to predict the backside wear [50]. To analyse a contact problem, master (target) and slave (contact) surfaces have to be defined. The master (target) surface is the surface of the "hard" material, for instance, acetabular head and shell; whereas the slave (contact) surface is the surface of the "soft" material e.g. UHMWPE liner.

2.7 Contact Algorithm

Contact is a changing-status nonlinearity and is implemented in an incremental manner [80]. There are generally three main aspects of the contact modelling algortihm: (1) identifying the area on the surfaces that are in contact; (2) calculating the contact force in the normal direction of the surfaces due to penetrations; (3) thereafter calculating the tangential force caused by friction. Since a surface point of a body is possible to contact any portion of the surface of another body; it can even come into contact with a part of the surface of its own body, search for correct location may require considerable effort. The search algorithms can be divided in two general approaches [81]. The first approach is for contact between a deformable and a rigid body, where the rigid body can be described as superquadrics or hyperquadrics [82], resulting simple and efficient contact search for surface points on the deformable body. The second approach is for contact amongst two or more deformation bodies or in the present of self-contact, where the search is more complex and normally split into a global and a local search [83]. The high computing cost but less frequently conducted global search is used to find out which bodies, parts of the bodies, surfaces or parts of the surfaces are able to come into contact within a given time step. Once the potential contacts are known, a less expensive local search is performed to determine if a penetration has occurred and its exact location. The penalty method has been applied in a number of THR wear FE studies to model the contact in normal direction. The normal contact force, which is calculated as the penetration distance multiplied by the penalty stiffness, is applied to the slave surface to resist its penetration to master surface. Simultaneously, opposite forces act on the master surface at the penetration point. The tangential motion will not start until the frictional shear stress reaches a critical value (τ_{crit}), which is defined by Coulomb friction model:

$$\tau_{crit} = \mu \cdot p \qquad (2)$$

where μ is the coefficient of friction and p is the normal contact pressure. If the shear stress is below τ_{crit}, there will no relative motion between the contact surfaces (sticking). While when the frictional shear stress reaches its critical value relative motion (slipping) occurs [55].

3. FEA Wear Modelling

Wear, progressive damage and material loss which occurs on the surface of a component as a result of its motion relative to the adjacent working parts [84], is widely recognised as the most important factor affecting the long term integrity of THRs. For this reason, it has been intensively investigated both experimentally and clinically, demonstrating the coexistence of abrasive, adhesive, fatigue and corrosive wear [42]. Instead of investigating and distinguishing these microscopic wear mechanisms, FEA modelling of wear to date has focused on reproducing the geometrical changes at the macroscopic scale.

3.1 Wear Law

Almost all of the numerical models on polyethylene liner wear prediction implemented the Archard's wear law [85], either in its original form [21-23, 46, 48, 50-54, 56-58, 61, 66, 69, 86-91] or modified forms [18, 19, 25, 31, 41, 49, 60, 65, 67, 68, 92, 93], mostly in commercial FEA software (e.g. Ansys or Abaqus) by means of user-defined routines. Due to its simplicity and validity, Archard's law has been widely used for many applications, despite the fact that it can only describe the adhesive and abrasive wear mechanisms [42]. After determining the contact pressure and sliding distance from the contact FEA at the end of each time increment, material loss resulting from wear is approximated by repositioning the contact nodes on the contact surface [80]. The new coordinates of each node are evaluated by shifting the node along the direction opposite to contact normal according to [94]

$$H = \sum_{i=1}^{n} K_i \sigma_i S_i \tag{3}$$

where H is the accumulated linear wear, K_i is the wear coefficient, σ_i is the contact pressure and S_i is the sliding distance at time increment of i.

It is unfeasible to update the bearing surface after each load cycle, due to the large number of cycles required to be simulated (1 million cycles per year is assumed in typical patients). The cumulative wear has been generally updated after a number of cycles, known as the update interval N_0 [48], which has varied from 0.1 million cycles [52], through 0.25 million cycles [49], to 0.5 million cycles [21, 53]. Both the linear wear and volumetric wear at the end of the interval are determined by multiplying by N_0.

3.2 Wear Coefficient

The wear coefficient is one the most critical inputs of wear modelling, and varies greatly as a function of a number of experimental variables including polyethylene molecular weight, lubricant fluid, counter-face material, roughness of the harder surface and sterilization method. Hence, a wide range of wear coefficients have been used in literature, as detailed in Table 2. Wear coefficients for the FEA wear prediction have been determined by two means: Pin-on-Disk and simulator studies. These each have their limitations: 1) Pin-on-Disk does not mimic the time dependent loading which the hip joint is subjected to *in vivo* [95] and thus some FEA wear predictions have varied considerably when compared to corresponding experimental results. 2) Simulator studies are not an independent verification as the wear coefficient is only valid for the single set of conditions applied [92]. Additional simulator testing is required when analysing different geometry designs even with the same bearing material and lubricant composition [27].

There have generally been four different forms of wear coefficients in the published FEA studies: 1) constant in space and time; 2) cross-shear dependent; 3) contact pressure dependent; 4)

surface roughness dependent. The majority of wear FEA models have used a constant wear coefficient, which has not accounted for the variation due to third-body particle wear, oxidation, cross shear, contact pressure, or surface roughness. To date there has not been general agreement regarding which form of the wear coefficient is the best in predicting UHMWPE liner wear and whether using the more complicated cross shear, pressure and roughness dependent wear coefficients actually improve the correlation with simulator wear testing results, as discussed in Section 3.2.1 − 3.2.3. Hence challenges remain to find a scientific approach for measuring and deriving a wear coefficient model for the FEA modelling of UHMWPE liner wear.

Table 2 Wear coefficients used in numerical study of UHMWPE liner wear

3.2.1   Cross Shear Effects

It has been identified that multi-directional or "cross-shear" motion is one of the most significant factors affecting the wear rate of UHMWPE liners in THR [96]. Under linear tracking motion, the molecules of polyethylene material are stretched along the sliding direction, resulting in a significant degree of strain hardening hence an increase of wear resistance in that direction [97]. However, strengthening in one direction leads to weakening in the transverse direction [98], known as orientation softening, which accelerates the wear debris generation.

The cross shear effect at a point on the bearing surface has been quantified by a Cross Shear Ratio (CSR). It was defined as the frictional work (W_T) in the direction perpendicular to the Principal Molecular Orientation (PMO) divided by the total frictional work (W_T+W_P), where W_P is the frictional work in the primary direction [67, 99]:

$$CSR = {W_T}/{(W_T + W_P)} \qquad (4)$$

According to the theory of Wang [97] the PMO was defined as the axis along which most the frictional work occurred. It was iteratively calculated by searching for the axis which gave the minimum CSR [67]. This approach was later adapted by a number of studies [25, 41, 49, 65]. However, by introducing cross shear dependent effects, the predicted wear rate only increased by 7.5%, from 24.7 mm^3/Mc (cross shear independent) to 26.7 mm^3/Mc (cross shear dependent), in the case study of a 28mm bearing [67]. It is worth noting that majority of the cross shear models were time independent, i.e. assuming that the molecular orientation remains fixed in a single direction over time, which may not be a clinical relevant representation [100]. Hence, time dependent cross shear models [31, 93] have been developed to improve the accuracy of wear prediction.

3.2.2 Contact Pressure Effects

The wear coefficient has been found to decrease when contact pressure increased according to Pin-on-Disk [95, 101-103] and simulator tests [78]. To take the effect of contact pressure into account, pressure-dependent wear coefficients have been employed in numerical studies [68, 79]. In addition, a wear coefficient model which is a two-dimensional function of the contact pressure and Cross Shear Ratio (CSR) has been used in one FEA study [92]. However, this under-predicted the volumetric wear rate by a factor of 2.8, when compared to hip simulator results. Alternatively, a contact area dependent wear model has been proposed [49, 60, 65], in which the wear is assumed to be independent of the contact pressure, and the volumetric wear (V) calculated by:

$$V = CAL \tag{5}$$

where C is a dimensionless constant, A is contact area and L is the sliding distance. The wear rate was improved but still underestimated by a factor of 1.7 [49]. Until now there is still controversy whether the contact pressure effects should be incorporated in numerical wear predictions [93].

3.2.3 Surface Roughness Effects

Instead of modifying the femoral head surface topography, the effects of head roughness on UHMWPE liner wear have been investigated by manipulating the wear coefficient. In some cases, the wear coefficient has been scaled over specific regions of the femoral head [56, 69], in order to investigate the influences of head roughening severity, roughened area size and roughened area location. In other cases, a roughness-dependent wear coefficient has been defined [18-20], where mathematical analyses have shown that UHMWPE wear is proportional to head surface roughness R_a, and confirmed by laboratory investigations [104, 105].

Furthermore, challenges remain to establish the effects of debris, lubrication regimes and frictional heating on wear coefficient. In both clinical and experimental situations, debris would still be in the vicinity of the joint space and at some point it may be pulled onto the bearing with entrained fluid. However, it would be very difficult to quantify this effect and hence make a meaningful modification to any wear models.

Theoretical prediction of lubrication regimes are usually defined by the lambda ratio λ [42]:

$$\lambda = \frac{h_{min}}{R_a} \tag{6}$$

where h_{min} corresponds to the minimum film thickness and R_a composites roughness of the bearing couple. Lubrication regime can be identified by the following ranges: 0.1<λ<1: boundary lubrication; 1≤λ≤3: mixed lubrication and λ>3: full film lubrication. Since the film thickness can be very close to the average roughness of articulating surfaces, even in simple daily activities mixed

and boundary lubrication may occur [106]. In these cases, bearing components enter in contact, consequently resulting in wear. Although a significant amount of research has been done studying lubrication and wear, they were modelled completely neglecting each other, as highlighted by the review of Mattei et al [42]. As such no wear coefficient models have been coupled with lubrication regimes.

Depending on magnitude, temperature increase due to frictional heating at the articulating interface may cause creep and oxidative degradation of UHMWPE liner material, degrade the mechanical properties of the lubricating fluid and further elevate wear generation as well as increase risk of damage surrounding tissues [107]. Currently, only Fialho et al [57] simultaneously modelled wear and heat generation in THR. However, the researchers employed a constant wear coefficient and their model could not explain the lack of correlation between temperature and contact pressure as observed *in vivo* [108].

3.3 Model Verification & Validation

It is critical to verify and validate the wear FEA model before it can provide guidance to testing, assist product development, and serve as valid scientific evidence in regulatory submissions [109]. Verification is defined as "the process of gathering evidence to establish that the computational implementation of the mathematical model and its associated solution are correct", while validation is "the process of determining the degree to which a model is an accurate representation of the real world from the perspective of the intended uses of the model" [110]. This has been summarised as verification being to "solve the equations right" (i.e. the mathematics) and validation being to "solve the right equations" (i.e. the physics) [111]. Verification may include examining both the code and the calculation. Code verification ensures the mathematical model and solution algorithm work as intended, usually by comparing the numerical solution with the exact analytical solutions or semi-analytical solutions [111]. In the papers reviewed, code verification was not explicitly reported; instead authors used proprietary software and existing codes where verification was assumed to have been undertaken by the manufacturer. Calculation verification focuses on errors resulting from discretisation of geometry and time domains, respectively, such as by means of mesh convergence study [22, 48, 54] and investigation of wear geometrical update interval [23, 48], aiming to achieve the desired computational accuracy while maintaining an acceptable computational efficiency. The mesh convergence studies [22, 48] may be limited as they were based on contact pressure results rather than wear results which can also be affected by nodal sliding distance and geometrical update, etc. To ensure that FEA wear prediction is independent of numerical settings, further sensitivity studies have been done on frictional coefficient [53, 54] and wear coefficient [68], as discussed in Section 2.6 and 3.2, respectively.

There are two predominant types of validation: direct and indirect. Direct validation aims to produce an experiment which closely matched the FE simulation so that its material property and

boundary condition can be incorporated [111]. This has been undertaken in the reviewed studies, for instance, by benchmarking the numerically predicted volumetric and linear wear (penetration) rate [21, 53, 67, 87] as well as wear cross-sectional profile [53, 69] against the corresponding hip simulator testing results. The results of these comparisons have shown that FE simulation has the potential to provide an excellent estimation of volumetric and linear wear rate. However, challenge remains to accurately capture the wear cross-sectional profile, for instance, two distinct surface damage peaks were found in experimental case whereas only a single damage peak was predicted by FEA [53]. Indirect validation compares the FEA results with published *in vivo* and *in vitro* wear data that cannot be controlled by the analyst. For example, some wear prediction were evaluated against the existing hip simulator tests [48, 49], FE wear predictions [48, 50, 57, 66, 68] or clinical studies [22, 54, 57, 58, 87, 91, 92]. Due to the fact that the sources of error and degree of variability in published investigations are typically unknown, indirect validation is clearly less favoured than direct validation. Hence, unless in the case of patient-specific study, wear FEA should be directly validated against well controlled experimental testing conditions, e.g. hip simulator testing, which employs the same geometry, loading and kinematics as FEA modelling. Indeed, this relies on the assumption that simulator testing is an accurate representation of the clinical situation, which has been discussed elsewhere and is not a consideration of this review. Table 3 details the input conditions, predicted wear rates and modal validation of the wear FEA studies which are reviewed in this paper.

Table 3 A summary of the input conditions, predicted wear rates from FEA studies of UHMWPE liners and modal validation

4. Mechanics of Wear and Creep

FEA modelling has the advantage of understanding the in-process mechanics of wear and creep, which might be difficult for laboratory analysis and clinical studies to accomplish, such as analysing the change of contact area, contact pressure and penetration over one loading cycle.

4.1 Wear Mechanics

Understanding the contact mechanics is important to gain insight into the wear generation of UHMWPE liner, as it determines the contact pressure and sliding distance, which are vital in the wear prediction based on Archard's law. The change of contact pressure within one load cycle corresponds to the load history applied, i.e. high pressure and large contact area were found in the stance phase while low pressure and small contact area occur in the swing phase of walking cycle, as reported by Matsoukas et al [53]. In addition, contact pressure decreases with the progression of wear, due to the resulting increase in contact area.

Wear has been found to be directly proportional to the contact area [49, 65, 103]. The wear contour of UHMWPE liner approximately follows the contact pressure distribution [48, 65].

13

Depending on the loads and motions being used in the FEA models, wear might occur within the superior half of the liner [57, 61] or in the superior-posterior region [21, 22, 67], emphasising the important effects of different individual gait cycles on the characteristics of wear. Due to the variation of load, motion, geometry and wear coefficients used, the predicted wear rates have differed considerably in various FEA models, as summarised in Table 3.

4.2 Creep Mechanics

Penetration of the femoral head into the acetabular cup caused by creep accounts for a considerable amount of the volumetric change of the UHMWPE liner [112, 113], especially in the initial loading stage, known as the "bedding-in" period, but it has little influence on the long term volumetric change [114-118]. The FEA study by Liu et al [65] showed that in the first million cycles creep contributed to approximately 80% of volumetric change and linear penetration. Then the creep remained almost the same and bearing geometry change was mainly the result of wear, as shown in Figure 6.

Figure 6 FEA prediction of creep, wear and total volume change. Reprinted from Liu et al [65], with permission from SAGE Publishing

Due to the existence of creep, volumetric wear assessment, e.g. using Coordinate Measuring Machine (CMM), and also any radiographic technique used clinically would almost certainly overestimate the true wear of a UHMWPE liner. The detrimental effects of wear are primarily related to the effects of the wear particles generated and so from a clinical perspective, it is of great interest to separate the bearing geometrical change due to creep to better evaluate true wear rate *in vivo*. The contours of the creep, wear and total penetration after 1 million cycle based on an early creep study by Bevill et al [51] are shown in Figure 7.

Figure 7 Contour plots showing the magnitude of creep, wear and total penetration after 1 million cycle, predicted using FEA. Reprinted from Bevill et al [51], with permission from Elsevier

Creep strain of UHMWPE material was found to be in linear relationship with time (logarithmic scale) and pressure [119]. It can be derived as equation (7) which has been used in all the creep and wear FEA of UHMWPE liners [51-53, 61, 65]:

$$\varepsilon_{cp} = A\sigma\log(t) \tag{7}$$

where ε_{cp} is the creep strain, A is a constant, e.g. 7.97/[log(min)]MPa [119], σ is the contact pressure and t is the time.

Creep has been shown to result in an increase in contact area and subsequent decrease in the contact pressure between the head and UHMWPE liner. The FEA study by Bevill et al [51] showed that creep increased the contact area by up to 56%, subsequently reducing contact pressure by up to 41%. Volumetric wear has been found to increase by 25% after five million cycles when creep was taken into account, compared to the FEA without creep [65], due to the increase in contact area resulting from the "bedding-in" at the articulating surface. Hence in order to accurately predict the wear of the UHMWPE liner, it may be necessary to include creep analysis, which however was not taken into account in the majority of wear FEA models to date. In addition, creep penetration was found to increase when decreasing head diameter or increasing bearing clearance [51], because both scenarios would cause an increase in the contact pressure which has a linear relationship to the creep strain.

5. Parametric Studies of Wear

To further understand the wear mechanics, optimise different parameters and ultimately determine how to minimise the UHMWPE liner wear, FEA studies have been carried out to investigate the effects of design parameters as well as surgical and patient parameters.

5.1 Effect of Design Parameters

5.1.1 Head Diameter

Femoral head size is one of the most studied parameters in FEA wear modelling of the UHMWPE liner. Early clinical practice tended to use smaller head diameters (22, 28mm). In contrast the current design of polyethylene bearings tends to use larger head diameters (32 or 36mm), aiming to achieve improved joint stability and range of motion [120]. However, a larger femoral head has been shown to induce a larger wear volume [18, 19, 21-23, 48, 49, 51, 52, 65, 86, 87] due to increase in contact area and sliding distance. By contrast, linear wear has been shown to decrease with increased of head diameter [23, 51, 52, 66, 86, 87], due to lower pressure at bearing surfaces.

5.1.2 Bearing Clearance

The interference between two articulating surfaces plays an important role in the wear process. In general, similar to the effect of using a small head, increasing the bearing clearance would also result in high contact pressure and low contact area. Hence it has been reported that large clearance was associated with increase in the linear wear [51] and decrease in the volumetric wear [48, 51, 65]. However, higher volumetric wear has also been found when using larger clearances [54]. The difference in outcome might be attributed to the fact that, in the latter study, Teoh et al [54] applied a perfect plasticity material model, which inevitably over-predicted the strain (deformation) of the liner when the stress exceeds the predefined yield limit. In the case of large clearance, plastic stress associated with the initial smaller contact area, permanently deformed the liner and increased the bearing contact area, leading to an over-prediction of the wear rate. It is also worth noting that investigating the effect of bearing clearance by using a constant wear coefficient might be of limited clinical relevance [51], considering that lubrication is in fact affected by bearing geometry and clearance.

5.1.3 Liner Thickness

The effects of UHMWPE liner thickness greater than 8mm on the contact and wear mechanics were generally negligible [19, 22]. In a study where the UHMWPE liner thickness was increased from 4 to 16 mm, volumetric wear was found to only increase slightly and there were modest effects on total penetration [51]. Maxian et al [21] reported that for a 22 mm and 32 mm bearing, the wear volume increased by 1.4% and 0.05%, respectively, when the liner thickness decreased from 10 to 2mm.

5.1.4 Screw Hole

The majority of FEA wear predictions focused on the articulating head/liner interface, which is the primary source of the UHMWPE wear. The only FEA wear study to investigate the liner/shell (backside) interface showed that the wear of the backside was 3-4 orders of magnitudes less than it at the head/liner (frontside) interface [50], primarily due to the difference in sliding distance of the two interfaces. Increasing the number of screw holes on the metal shell was found to reduce the backside wear but had negligible effects on the frontside wear [50]. It is worth noting that this study was limited to initial wear rates with a polished backside interface; however long term backside wear in the presence of screws and screw holes may still influence the clinical performance of artificial hip joints [121, 122].

5.1.5 Liner/Shell Conformity

Liner/shell nonconformity may be present by design, due to the incorporation of locking mechanisms to attach the UHMWPE liner to the metal shell, or limitations on UHMWPE liner

manufacturing tolerances [123]. In the FEA model of Kurtz et al [50], a radial clearance of 0.223mm was used in the spherical region of the interface to simulate the nonconformity. In general, the nonconforming shell was found to produce higher linear wear and lower volumetric wear at the backside interface. By contrast, wear results of the frontside interface have shown to be insensitive to the shell conformity [50].

5.2 Effect of Surgical and Patient Parameters

5.2.1 Cup Positioning

Component positioning of an artificial hip joint plays a key role in patient's mobility and the durability of the implant [66]. Steep inclination angles have been shown to cause the contact area to decrease and shift to the edge of the cup [58, 124], consequently increase the contact stress [124-126]. According to several numerical studies, higher cup inclination angles result in higher linear wear [58, 88, 91] due to high contact stress, but lower volumetric wear [18, 19, 58, 127] resulting from reduced contact area (sliding distance), as is in agreement with some hip simulator testing [128, 129]. However, higher volumetric wear has been observed with higher inclination angles in other clinical [15], hip simulator [88, 130] and FEA modelling studies [91]. Further investigation is hence necessary to understand the difference amongst various FEA, laboratory and clinical studies, especially under the edge loading condition induced by steep cup inclination and lateral separation. Additionally, it has been reported that an increased cup anteversion angle would cause wear volume to increase, according to a mathematical prediction [19].

5.2.2 Motion Input

It is widely recognised that multidirectional motion in a joint simulator yields realistic wear for the UHMWPE liner [131]. However, the type of motion inputs has varied considerably amongst simulators, which may explain the differences in wear rate [132]. The importance of articulation kinematics has also been emphasised in the FEA of wear [21], where a 23° biaxial rocking simulator inputs [133] resulted in an increase of wear rate of 1.7 times compared to human gait inputs [134]. Recently, the numerically predicted wear results under three motion inputs have been compared [60], and it was found that volumetric wear rates of the simplified walking condition including ISO14242 [64] and Leeds ProSim simulator [65] were 4% and 13% lower respectively, compared with that of the full simulated condition based on a gait measurement [135]. In contrast, the linear wear was similar when using those three motion inputs.

5.2.3 Daily Activity

So far, almost all FEA studies have focused on wear prediction under a normal walking condition, as listed in Table 3. Few attempts have been made to model UHMWPE liner wear due to running, descending or ascending stairs. In a mathematical study by Pietrabissa et al [18] wear volume

increased with a rise in walking speed and decreased slightly when running at the same speed. In contrast an FEA study by Fialho et al [57] reported an almost doubling of the wear rate in a running cycle compared to a walking cycle. This was associated with a dramatic increase in loading [57], while the speeds of those cycles were not specified. The same study [57] also showed that wear results for walking in two different patients varied significantly, primarily due to variation of loading and sliding distance as measured clinically by Bergmann et al [136]. In other studies, higher wear was predicted under the conditions of descending stairs [79] and ascending stairs [53, 79] versus normal walking, due to the higher range of motion involved in ascending stairs than walking [61]. Combined walking and stair ascending were found to produce higher volumetric wear than walking alone [56].

5.2.4   Body Weight

According to Archard's law, wear is proportional to the load applied. The mathematically predicted wear was found to increase linearly with body weight [18-20], and is in agreement with one clinical study [137]. However, other clinical studies have found no such correlation between patient's weight and clinical wear rate [138-140]. A possible explanation for this may be that patient weight and activity may not be independent factors. For example some heavier patients may be less active than those who are lighter.

6. Discussion

Due to the variation of load, motion, geometry and wear coefficient inputs, the predicted wear rates were found to differ considerably across the various FEA models studied. Further work should explore the influences of different meshing methods, the use of the explicit solution method, and 3D vs. 1D loading and motion in the FEA modelling technique. Moreover, challenges remain to find a scientific approach to measure and derive wear coefficients. It is critical to validate the FEA model before it can provide guidance to testing and assist product development.

Creep can account for a considerable amount of the volumetric change of UHMWPE liner, especially in the initial loading stage. Due to the increase of contact area resulting from the "bedding in", the wear rate of an UHMWPE liner could increase considerably. Hence it is likely to be necessary to include creep analysis in the wear simulation. This will be especially true if comparisons are being made to simulator or clinical data which have used volumetric measurements.

A number of parametric studies have been carried out to numerically investigate the effects of design, surgical and patient parameters on the UHMWPE liner wear. The effect of cup positioning is still not fully understood, especially under the edge loading condition associated with steep cup inclination and lateral separation. Future FEA work could employ Design of Experiment methods

to understand the interaction amongst the multiple factors and derive optimised settings to minimise the wear.

The majority of the FEA studies focused on wear prediction under a normal walking condition. A significant knowledge gap still exists in studying other daily actives, such as cycling, sitting down and getting up a chair, etc. Furthermore, a statistical methodology might be needed to combine a number of activities in order to estimate wear during a "realistic" daily life, rather than just investigating one activity alone.

All FEA wear modelling of UHMWPE liner wear simulate the dry contact between articulating surfaces, by neglecting the lubrication. Further development could employ Fluid-Structure Interaction techniques, in order to take the effects of lubrication into account.

7. Conclusion

Recent developments in understanding of variable outcomes in hip replacement have led to an increasing need for development of wear simulation methods which address more complex surgical and patient scenarios. Carrying out multi-factorial clinical and laboratory studies with material, design, manufacturing and surgical-patient parameters makes the cost and time for developing implants unrealistic. To address the challenges and limitations, FEA simulation on UHMWPE liner wear in THR has been under development since the 1990s because it is an efficient and inexpensive approach to predict wear and provide initial screening of various parameters. The present paper is a comprehensive literature review on the state-of-the-art FEA modelling techniques, wear mechanics, and parametric studies of UHMWPE liner wear. A number of knowledge gaps have been identified for future studies, such as further development of wear coefficient models, creep modelling, Design of Experiments, optimisation of cup positioning, study of edge loading conditions, analysis of the activities of daily living and implementation of Fluid-Structure Interactions. The further development and use of FEA has the potential to make the comprehensive testing of new materials and designs a practical proposition. It offers an approach to gain in-depth understanding of wear mechanics, to deliver guidelines for new product design, and to assist pre-surgical planning.

8. Conflict of Interest
None declared.

9. Acknowledgement

10. Reference

1. Affatato, S., *1 - The history of total hip arthroplasty (THA)*, in *Perspectives in Total Hip Arthroplasty*. 2014, Woodhead Publishing. p. 3-18.
2. Ingham, E. and J. Fisher, *Biological reactions to wear debris in total joint replacement.* Proceedings of the Institution of Mechanical Engineers, Part H: Journal of Engineering in Medicine, 2000. **214**(1): p. 21-37.
3. Sloten, J.V., et al., *Materials selection and design for orthopaedic implants with improved long-term performance.* Biomaterials, 1998. **19**(16): p. 1455-1459.
4. Kurtz, S.M., et al., *Advances in the processing, sterilization, and crosslinking of ultra-high molecular weight polyethylene for total joint arthroplasty.* Biomaterials, 1999. **20**(18): p. 1659-1688.
5. Affatato, S., *8 - Tribological interactions of polyethylene in total hip arthroplasty (THA)*, in *Perspectives in Total Hip Arthroplasty*. 2014, Woodhead Publishing. p. 117-126.
6. Kurtz, S.M., H.A. Gawel, and J.D. Patel, *History and Systematic Review of Wear and Osteolysis Outcomes for First-generation Highly Crosslinked Polyethylene.* Clinical Orthopaedics and Related Research®, 2011. **469**(8): p. 2262-2277.
7. Affatato, S., *7 - Tribological interactions of modern biomaterials used in total hip arthroplasty (THA)*, in *Perspectives in Total Hip Arthroplasty*. 2014, Woodhead Publishing. p. 99-116.
8. Hadley, M.J.F., *Long term functional simulation of large diameter metal on metal hip implants*. 2012: University of Leeds.
9. Hadley, M., et al. *In-vitro wear simulation of different materials for total hip replacement under stop-dwell-start conditions*.
10. Yeung, E., et al., *The effect of obesity on the outcome of hip and knee arthroplasty.* International Orthopaedics, 2011. **35**(6): p. 929-934.
11. McClung, C.D., et al., *Relationship between body mass index and activity in hip or knee arthroplasty patients.* Journal of Orthopaedic Research, 2000. **18**(1): p. 35-39.
12. Fisher, J., *Bioengineering reasons for the failure of metal-on-metal hip prostheses.* Journal of Bone &amp; Joint Surgery, British Volume, 2011. **93-B**(8): p. 1001.
13. Harris, W.H., *Edge Loading Has a Paradoxical Effect on Wear in Metal-on-Polyethylene Total Hip Arthroplasties.* Clinical Orthopaedics and Related Research®, 2012. **470**(11): p. 3077-3082.
14. Sakalkale, D.P., et al., *Effect of femoral component offset on polyethylene wear in total hip arthroplasty.* Clinical orthopaedics and related research, 2001. **388**: p. 125-134.
15. Little, N.J., et al., *Acetabular polyethylene wear and acetabular inclination and femoral offset.* Clinical Orthopaedics and Related Research, 2009. **467**(11): p. 2895-2900.
16. Bhaskar, D., A. Rajpura, and T. Board, *Current Concepts in Acetabular Positioning in Total Hip Arthroplasty.* Indian Journal of Orthopaedics, 2017. **51**(4): p. 386-396.
17. De Fine, M., et al., *Is there a role for femoral offset restoration during total hip arthroplasty? A systematic review.* Orthopaedics & Traumatology: Surgery & Research, 2017. **103**(3): p. 349-355.
18. Pietrabissa, R., M. Raimondi, and E. Di Martino, *Wear of polyethylene cups in total hip arthroplasty: A parametric mathematical model.* Medical Engineering and Physics, 1998. **20**(3): p. 199-210.
19. Raimondi, M.T., et al., *Improved mathematical model of the wear of the cup articular surface in hip joint prostheses and comparison with retrieved components.* Proceedings of the Institution of Mechanical Engineers, Part H: Journal of Engineering in Medicine, 2001. **215**(4): p. 377-390.
20. Mattei, L., F. Di Puccio, and E. Ciulli, *A comparative study of wear laws for soft-on-hard hip implants using a mathematical wear model.* Tribology International, 2013. **63**(Supplement C): p. 66-77.

21. Maxian, T.A., et al., *3-Dimensional sliding/contact computational simulation of total hip wear.* Clinical Orthopaedics and Related Research, 1996(333): p. 41-50.

22. Maxian, T.A., et al., *A sliding-distance-coupled finite element formulation for polyethylene wear in total hip arthroplasty.* Journal of Biomechanics, 1996. **29**(5): p. 687-692.

23. Maxian, T.A., et al., *Adaptive finite element modeling of long-term polyethylene wear in total hip arthroplasty.* Journal of Orthopaedic Research, 1996. **14**(4): p. 668-675.

24. Abdelgaied, A., et al., *The effect of insert conformity and material on total knee replacement wear.* Proceedings of the Institution of Mechanical Engineers, Part H: Journal of Engineering in Medicine, 2014. **228**(1): p. 98-106.

25. Abdelgaied, A., et al., *Computational wear prediction of artificial knee joints based on a new wear law and formulation.* Journal of Biomechanics, 2011. **44**(6): p. 1108-1116.

26. Innocenti, B., et al., *Development and Validation of a Wear Model to Predict Polyethylene Wear in a Total Knee Arthroplasty: A Finite Element Analysis.* Lubricants, 2014. **2**(4).

27. O'Brien, S., et al., *Computational development of a polyethylene wear model for the articular and backside surfaces in modular total knee replacements.* Tribology International, 2013. **59**: p. 284-291.

28. Willing, R. and I.Y. Kim, *Three dimensional shape optimization of total knee replacements for reduced wear.* Structural and Multidisciplinary Optimization, 2009. **38**(4): p. 405-414.

29. Zhang, J., et al., *A patient-specific wear prediction framework for an artificial knee joint with coupled musculoskeletal multibody-dynamics and finite element analysis.* Tribology International, 2017. **109**: p. 382-389.

30. Zhao, D., et al., *Predicting Knee Replacement Damage in a Simulator Machine Using a Computational Model With a Consistent Wear Factor.* Journal of Biomechanical Engineering, 2008. **130**(1): p. 011004-011004-10.

31. O'Brien, S.T., et al., *An energy dissipation and cross shear time dependent computational wear model for the analysis of polyethylene wear in total knee replacements.* Journal of Biomechanics, 2014. **47**(5): p. 1127-1133.

32. Mattei, L., et al., *Numerical and experimental investigations for the evaluation of the wear coefficient of reverse total shoulder prostheses.* Journal of the Mechanical Behavior of Biomedical Materials, 2016. **55**: p. 53-66.

33. Mattei, L., et al., *Effect of size and dimensional tolerance of reverse total shoulder arthroplasty on wear: An in-silico study.* Journal of the Mechanical Behavior of Biomedical Materials, 2016. **61**: p. 455-463.

34. Terrier, A., et al., *Comparison of polyethylene wear in anatomical and reversed shoulder prostheses.* The Journal of Bone and Joint Surgery. British volume, 2009. **91-B**(7): p. 977-982.

35. Quental, C., et al., *Computational analysis of polyethylene wear in anatomical and reverse shoulder prostheses.* Medical & Biological Engineering & Computing, 2015. **53**(2): p. 111-122.

36. Ribeiro, N.S., et al., *Wear analysis in anatomical and reversed shoulder prostheses.* Computer Methods in Biomechanics and Biomedical Engineering, 2011. **14**(10): p. 883-892.

37. Gundapaneni, D., et al., *Wear characteristics of WSU total ankle replacement devices under shear and torsion loads.* Journal of the Mechanical Behavior of Biomedical Materials, 2015. **44**: p. 202-223.

38. Kerschhofer, D., et al., *Applicability of PEEK and its composites in total ankle replacement devices and wear rate predictions.* Biomedical Physics & Engineering Express, 2016. **2**(6): p. 065012.

39. Jay Elliot, B., D. Gundapaneni, and T. Goswami, *Finite element analysis of stress and wear characterization in total ankle replacements.* Journal of the Mechanical Behavior of Biomedical Materials, 2014. **34**: p. 134-145.

40. Jeremy, J.R., et al., *Wear simulation of the ProDisc-L disc replacement using adaptive finite element analysis.* Journal of Neurosurgery: Spine SPI, 2007. **7**(2): p. 165-173.
41. Goreham-Voss, C.M., et al., *Cross-shear implementation in sliding-distance-coupled finite element analysis of wear in metal-on-polyethylene total joint arthroplasty: Intervertebral total disc replacement as an illustrative application.* Journal of Biomechanics, 2010. **43**(9): p. 1674-1681.
42. Mattei, L., et al., *Lubrication and wear modelling of artificial hip joints: A review.* Tribology International, 2011. **44**(5): p. 532-549.
43. Liu, G.R. and S.S. Quek, *The Finite Element Method: A Practical Course*. 2013: Elsevier Science.
44. Rao, S.S., *The Finite Element Method in Engineering*. 2010: Elsevier Science.
45. Taylor, M. and P.J. Prendergast, *Four decades of finite element analysis of orthopaedic devices: Where are we now and what are the opportunities?* Journal of Biomechanics, 2015. **48**(5): p. 767-778.
46. Maxian, T.A., et al., *Finite element analysis of acetabular wear: Validation, and backing and fixation effects.* Clinical Orthopaedics and Related Research, 1997(344): p. 111-117.
47. Barreto, S., et al., *The influence of the pelvic bone on the computational results of the acetabular component of a total hip prosthesis.* Journal of Biomechanical Engineering, 2010. **132**(5).
48. Kang, L., et al., *A simple fully integrated contact-coupled wear prediction for ultra-high molecular weight polyethylene hip implants.* Proceedings of the Institution of Mechanical Engineers. Part H, Journal of engineering in medicine, 2006. **220**(1): p. 33-46.
49. Liu, F., et al., *A New Formulation for the Prediction of Polyethylene Wear in Artificial Hip Joints.* Proceedings of the Institution of Mechanical Engineers, Part H: Journal of Engineering in Medicine, 2010. **225**(1): p. 16-24.
50. Kurtz, S.M., et al., *Simulation of initial frontside and backside wear rates in a modular acetabular component with multiple screw holes.* Journal of Biomechanics, 1999. **32**(9): p. 967-976.
51. Bevill, S.L., et al., *Finite element simulation of early creep and wear in total hip arthroplasty.* Journal of Biomechanics, 2005. **38**(12): p. 2365-2374.
52. Penmetsa, J.R., et al., *Influence of polyethylene creep behavior on wear in total hip arthroplasty.* Journal of Orthopaedic Research, 2006. **24**(3): p. 422-427.
53. Matsoukas, G., R. Willing, and I.Y. Kim, *Total hip wear assessment: A comparison between computational and in vitro wear assessment techniques using ISO 14242 loading and kinematics.* Journal of Biomechanical Engineering, 2009. **131**(4).
54. Teoh, S.H., W.H. Chan, and R. Thampuran, *An elasto-plastic finite element model for polyethylene wear in total hip arthroplasty.* Journal of Biomechanics, 2002. **35**(3): p. 323-330.
55. *Abaqus documentation: analysis user's guide. v6.14*.
56. Lundberg, H.J., et al., *Nonidentical and outlier duty cycles as factors accelerating UHMWPE wear in THA: A finite element exploration.* Journal of Orthopaedic Research, 2007. **25**(1): p. 30-43.
57. Fialho, J.C., et al., *Computational hip joint simulator for wear and heat generation.* Journal of Biomechanics, 2007. **40**(11): p. 2358-2366.
58. Lin, Y.T., J.S.S. Wu, and J.H. Chen, *The study of wear behaviors on abducted hip joint prostheses by an alternate finite element approach.* Computer Methods and Programs in Biomedicine, 2016. **131**: p. 143-155.
59. Rimnac, C.M., et al., *Chemical and mechanical degradation of UHMWPE: Report of the development of an in vitro test.* Journal of applied biomaterials, 1994. **5**(1): p. 17-21.
60. Liu, F., J. Fisher, and Z. Jin, *Effect of motion inputs on the wear prediction of artificial hip joints.* Tribology International, 2013. **63**: p. 105-114.
61. Matsoukas, G. and I.Y. Kim, *Design optimization of a total hip prosthesis for wear reduction.* Journal of Biomechanical Engineering, 2009. **131**(5).

62. Cripton, P.A., *Compressive characterization of ultra high molecular weight polyethylene with applications to contact stress analysis of total knee replacements*. 1993.

63. Bergmann, G., et al., *Hip contact forces and gait patterns from routine activities.* Journal of Biomechanics, 2001. **34**(7): p. 859-871.

64. *ISO 14242-1:2002, Implants for surgery—wear of total hip-joint prostheses—part 1:*, in *loading and displacement parameters for wear-testing machines and corresponding environmental conditions for test.* . 2002.

65. Liu, F., J. Fisher, and Z. Jin, *Computational modelling of polyethylene wear and creep in total hip joint replacements: Effect of the bearing clearance and diameter.* Proceedings of the Institution of Mechanical Engineers, Part J: Journal of Engineering Tribology, 2012. **226**(6): p. 552-563.

66. Rońda, J. and P. Wojnarowski, *Analysis of wear of polyethylene hip joint cup related to its positioning in patient's body.* Acta of Bioengineering and Biomechanics, 2013. **15**(1): p. 77-86.

67. Kang, L., et al., *Wear simulation of ultra-high molecular weight polyethylene hip implants by incorporating the effects of cross-shear and contact pressure.* Proceedings of the Institution of Mechanical Engineers, Part H: Journal of Engineering in Medicine, 2008. **222**(7): p. 1049-1064.

68. Pakhaliuk, V., et al. *Improving the finite element simulation of wear of total hip prosthesis' spherical joint with the polymeric component*. in *Procedia Engineering*. 2015.

69. Brown, T.D., et al., *Local head roughening as a factor contributing to variability of total hip wear: A finite element analysis.* Journal of Biomechanical Engineering, 2002. **124**(6): p. 691-698.

70. Harewood, F.J. and P.E. McHugh, *Comparison of the implicit and explicit finite element methods using crystal plasticity.* Computational Materials Science, 2007. **39**(2): p. 481-494.

71. Godest, A.C., et al., *Simulation of a knee joint replacement during a gait cycle using explicit finite element analysis.* Journal of Biomechanics, 2002. **35**(2): p. 267-275.

72. Halloran, J.P., A.J. Petrella, and P.J. Rullkoetter, *Explicit finite element modeling of total knee replacement mechanics.* Journal of Biomechanics, 2005. **38**(2): p. 323-331.

73. Kang, K.T., et al., *Gait cycle comparions of cruciate sacrifice for total knee design.-explicit finite element.* International Journal of Precision Engineering and Manufacturing, 2012. **13**(11): p. 2043-2049.

74. Srinivas, G.R., A. Deb, and M.N. Kumar, *A study on polyethylene stresses in mobile-bearing and fixed-bearing total knee arthroplasty (TKA) using explicit finite element analysis.* Journal of Long-Term Effects of Medical Implants, 2013. **23**(4): p. 275-283.

75. Naghibi Beidokhti, H., et al., *A comparison between dynamic implicit and explicit finite element simulations of the native knee joint.* Medical Engineering and Physics, 2016. **38**(10): p. 1123-1130.

76. Ali, M. and K. Mao, *Contact mechanics and wear simulations of hip resurfacing devices using computational methods*. 2014: Acta of Bioengineering and Biomechanics. p. 103-110.

77. Gao, Y., J. Zhang, and Z. Jin, *Explicit finite element modeling of kinematics and contact mechanics of artificialhip and knee joints*. 2015: The 14th IFToMM World Congress, Taipei, Taiwan, October 25-30, 2015.

78. Wang, A., A. Essner, and R. Klein, *Effect of contact stress on friction and wear of ultra-high molecular weight polyethylene in total hip replacement.* Proceedings of the Institution of Mechanical Engineers, Part H: Journal of Engineering in Medicine, 2001. **215**(2): p. 133-139.

79. ONIŞORU, J., L. CAPITANU, and A. IAROVICI, *PREDICTION OF WEAR OF ACETABULUM INSERTS DUE TO MULTIPLE HUMAN ROUTINE ACTIVITIES* 2006: THE ANNALS OF UNIVERSITY "DUNĂREA DE JOS " OF GALAŢI FASCICLE VIII, 2006 (XII), ISSN 1221-4590 TRIBOLOGY. p. 28-33.

80. *Ansys documentation: mechanical APDL theory reference. v16.1*.

81. Wriggers, P., *Finite element algorithms for contact problems.* Archives of Computational Methods in Engineering, 1995. **2**(4): p. 1-49.

82.   John R, W. and P. Alex P, *SUPERQUADRICS AND MODAL DYNAMICS FOR DISCRETE ELEMENTS IN INTERACTIVE DESIGN.* Engineering Computations, 1992. **9**(2): p. 115-127.

83.   Zhong, Z.H., *Finite Element Procedures for Contact-impact Problems*. 1993: Oxford University Press.

84.   Williams, J., *Engineering Tribology*. Engineering Tribology. 1994: Cambridge University Press.

85.   Archard, J.F., *Contact and Rubbing of Flat Surfaces.* Journal of Applied Physics, 1953. **24**(8): p. 981-988.

86.   Hung, J.P. and J.S.S. Wu, *A comparative study on wear behavior of hip prosthesis by finite element simulation.* Biomedical Engineering - Applications, Basis and Communications, 2002. **14**(4): p. 139-148.

87.   Wu, J.S.S., et al., *The computer simulation of wear behavior appearing in total hip prosthesis.* Computer Methods and Programs in Biomedicine, 2003. **70**(1): p. 81-91.

88.   Patil, S., et al., *Polyethylene wear and acetabular component orientation.* Journal of Bone and Joint Surgery - Series A, 2003. **85**(SUPPL. 4): p. 56-63.

89.   Sfantos, G.K. and M.H. Aliabadi, *A boundary element formulation for three-dimensional sliding wear simulation.* Wear, 2007. **262**(5-6): p. 672-683.

90.   Sfantos, G.K. and M.H. Aliabadi, *Total hip arthroplasty wear simulation using the boundary element method.* Journal of Biomechanics, 2007. **40**(2): p. 378-389.

91.   Queiroz, R.D., et al., *A finite element method approach to compare the wear of acetabular cups in polyethylene according to their lateral tilt in relation to the coronal plane.* Wear, 2013. **298–299**: p. 8-13.

92.   Kang, L., et al., *Enhanced computational prediction of polyethylene wear in hip joints by incorporating cross-shear and contact pressure in additional to load and sliding distance: Effect of head diameter.* Journal of Biomechanics, 2009. **42**(7): p. 912-918.

93.   Strickland, M.A., M.R. Dressler, and M. Taylor, *Predicting implant UHMWPE wear in-silico: A robust, adaptable computational–numerical framework for future theoretical models.* Wear, 2012. **274-275**: p. 100-108.

94.   Marshek, K.M. and H.H. Chen, *Discretization Pressure-Wear Theory for Bodies in Sliding Contact.* Journal of Tribology, 1989. **111**(1): p. 95-100.

95.   Barbour, P.S.M., D.C. Barton, and J. Fisher, *The influence of contact stress on the wear of UHMWPE for total replacement hip prostheses.* Wear, 1995. **181–183, Part 1**: p. 250-257.

96.   Turell, M., A. Wang, and A. Bellare, *Quantification of the effect of cross-path motion on the wear rate of ultra-high molecular weight polyethylene.* Wear, 2003. **255**(7-12): p. 1034-1039.

97.   Wang, A., *A unified theory of wear for ultra-high molecular weight polyethylene in multi-directional sliding.* Wear, 2001. **248**(1–2): p. 38-47.

98.   Wang, A., et al., *Orientation softening in the deformation and wear of ultra-high molecular weight polyethylene.* Wear, 1997. **203–204**: p. 230-241.

99.   Kang, L., et al., *Quantification of the effect of cross-shear on the wear of conventional and highly cross-linked UHMWPE.* Journal of Biomechanics, 2008. **41**(2): p. 340-346.

100.   Dressler, M.R., et al., *Predicting wear of UHMWPE: Decreasing wear rate following a change in direction.* Wear, 2011. **271**(11): p. 2879-2883.

101.   Vassiliou, K. and A. Unsworth, *Is the wear factor in total joint replacements dependent on the nominal contact stress in ultra-high molecular weight polyethylene contacts?* Proceedings of the Institution of Mechanical Engineers, Part H: Journal of Engineering in Medicine, 2004. **218**(2): p. 101-107.

102.   Saikko, V., *Effect of contact pressure on wear and friction of ultra-high molecular weight polyethylene in multidirectional sliding.* Proceedings of the Institution of Mechanical Engineers, Part H: Journal of Engineering in Medicine, 2006. **220**(7): p. 723-731.

103. Fisher, J., et al., *2009 Knee Society Presidential Guest Lecture: Polyethylene Wear in Total Knees.* Clinical Orthopaedics and Related Research®, 2009. **468**(1): p. 12.

104. Lancaster, J.G., et al., *The wear of ultra-high molecular weight polyethylene sliding on metallic and ceramic counterfaces representative of current femoral surfaces in joint replacement.* Proceedings of the Institution of Mechanical Engineers, Part H: Journal of Engineering in Medicine, 1997. **211**(1): p. 17-24.

105. Welghtman, B. and D. Light, *The effect of the surface finish of alumina and stainless steel on the wear rate of UHMW polyethylene.* Biomaterials, 1986. **7**(1): p. 20-24.

106. Askari, E., et al., *A review of squeaking in ceramic total hip prostheses.* Tribology International, 2016. **93**: p. 239-256.

107. Uddin, M.S. and P. Majewski, *Frictional Heating in Hip Implants – A Review.* Procedia Engineering, 2013. **56**: p. 725-730.

108. Bergmann, G., et al., *Frictional heating of total hip implants, Part 1: measurements in patients.* Journal of Biomechanics, 2001. **34**(4): p. 421-428.

109. *ASME V&V 40: Assessing Credibility of Computational Modeling through Verification and Validation: Application to Medical Devices*. 2018, American Society of Mechanical Engineers.

110. *ASME V&V 10: Guide for verification and validation in computational solid dynamics*. 2006, American Society of Mechanical Engineers.

111. Henninger, H.B., et al., *Validation of Computational Models in Biomechanics.* Proceedings of the Institution of Mechanical Engineers. Part H, Journal of engineering in medicine, 2010. **224**(7): p. 801-812.

112. Isaac, G.H., D. Dowson, and B.M. Wroblewski, *An Investigation into the Origins of Time-Dependent Variation in Penetration Rates with Charnley Acetabular Cups—Wear, Creep or Degradation?* Proceedings of the Institution of Mechanical Engineers, Part H: Journal of Engineering in Medicine, 1996. **210**(3): p. 209-216.

113. Ramamurti, B.S., et al. *Dimensional changes in metal-backed polyethylene acetabular cups under cyclic loading*.

114. Wroblewski, B.M., et al., *PROSPECTIVE CLINICAL AND JOINT SIMULATOR STUDIES OF A NEW TOTAL HIP ARTHROPLASTY USING ALUMINA CERAMIC HEADS AND CROSS-LINKED POLYETHYLENE CUPS.* Journal of Bone &amp; Joint Surgery, British Volume, 1996. **78-B**(2): p. 280.

115. Dai, X., et al., *Serial Measurement of Polyethylene Wear of Well-Fixed Cementless Metal-Backed Acetabular Component in Total Hip Arthroplasty: An Over 10 Year Follow-up Study.* Artificial Organs, 2000. **24**(9): p. 746-751.

116. Pedersen, D.R., et al., *Comparison of femoral head penetration rates between cementless acetabular components with 22-mm and 28-mm heads.* The Journal of Arthroplasty, 2001. **16**(8): p. 111-115.

117. Devane, P.A. and J.G. Horne, *Assessment of Polyethylene Wear in Total Hip Replacement.* Clinical Orthopaedics and Related Research, 1999. **369**.

118. J. Sychterz, C., J.C. Engh, and A. Yang, *Analysis of Temporal Wear Patterns of Porous-Coated Acetabular Components: Distinguishing Between True Wear and So-Called Bedding-in**. Vol. 81. 1999. 821-30.

119. Lee, K.Y. and D. Pienkowski, *Compressive creep characteristics of extruded ultrahigh-molecular-weight polyethylene.* Journal of Biomedical Materials Research, 1998. **39**(2): p. 261-265.

120. Burroughs, B.R., et al., *Range of Motion and Stability in Total Hip Arthroplasty With 28-, 32-, 38-, and 44-mm Femoral Head Sizes: An In Vitro Study.* The Journal of Arthroplasty, 2005. **20**(1): p. 11-19.

121. Bloebaum, R.D., et al., *Postmortem analysis of bone growth into porous-coated acetabular components.* J Bone Joint Surg Am, 1997. **79**(7): p. 1013-22.
122. Huk, O.L., et al., *Polyethylene and metal debris generated by non-articulating surfaces of modular acetabular components.* Bone & Joint Journal, 1994. **76**(4): p. 568-574.
123. Kurtz, S.M., et al., *Backside nonconformity and locking restraints affect liner/shell load transfer mechanisms and relative motion in modular acetabular components for total hip replacement.* Journal of Biomechanics, 1998. **31**(5): p. 431-437.
124. Hua, X., et al., *Contact mechanics of modular metal-on-polyethylene total hip replacement under adverse edge loading conditions.* Journal of Biomechanics, 2014. **47**(13): p. 3303-3309.
125. D'Lima, D.D., P.C. Chen, and C.W. Colwell, *Optimizing acetabular component position to minimize impingement and reduce contact stress.* The Journal of bone and joint surgery. American volume, 2001. **83-A Suppl 2 Pt 2**: p. 87-91.
126. Korhonen, R.K., et al., *The effect of geometry and abduction angle on the stresses in cemented UHMWPE acetabular cups – finite element simulations and experimental tests.* BioMedical Engineering OnLine, 2005. **4**(1): p. 32.
127. Rijavec, B., et al., *Effect of cup inclination on predicted contact stress-induced volumetric wear in total hip replacement.* Computer Methods in Biomechanics and Biomedical Engineering, 2015. **18**(13): p. 1468-1473.
128. Halma, J.J., et al., *Edge loading does not increase wear rates of ceramic-on-ceramic and metal-on-polyethylene articulations.* Journal of Biomedical Materials Research Part B: Applied Biomaterials, 2014. **102**(8): p. 1627-1638.
129. Korduba, L.A., et al., *Effect of acetabular cup abduction angle on wear of ultrahigh-molecular-weight polyethylene in hip simulator testing.* American journal of orthopedics (Belle Mead, N.J.), 2014. **43**(10): p. 466-471.
130. Ali, M., et al., *WEAR AND DEFORMATION OF METAL-ON-POLYETHYLENE HIP REPLACEMENTS UNDER EDGE LOADING CONDITIONS DUE TO VARIATIONS IN SURGICAL POSITIONING.* Bone & Joint Journal Orthopaedic Proceedings Supplement, 2017. **99-B**(SUPP 3): p. 12.
131. Saikko, V. and O. Calonius, *Slide track analysis of the relative motion between femoral head and acetabular cup in walking and in hip simulators.* Journal of Biomechanics, 2002. **35**(4): p. 455-464.
132. Ali, M., et al., *Influence of hip joint simulator design and mechanics on the wear and creep of metal-on-polyethylene bearings.* Proceedings of the Institution of Mechanical Engineers, Part H: Journal of Engineering in Medicine, 2016. **230**(5): p. 389-397.
133. Mejia, L.C. and T.J. Brierley, *A hip wear simulator for the evaluation of biomaterials in hip arthroplasty components.* Bio-medical materials and engineering, 1994. **4**(4): p. 259-271.
134. Brand, R.A., et al., *Comparison of hip force calculations and measurements in the same patient.* The Journal of Arthroplasty, 1994. **9**(1): p. 45-51.
135. Johnston, R.C. and G.L. Smidt, *Measurement of hip-joint motion during walking. Evaluation of an electrogoniometric method.* Journal of Bone and Joint Surgery - Series A, 1969. **51**(6): p. 1082-1094.
136. Bergmann, G., F. Graichen, and A. Rohlmann, *Hip joint loading during walking and running, measured in two patients.* Journal of Biomechanics, 1993. **26**(8): p. 969-990.
137. Gómez-Barrena, E., et al., *Role of polyethylene oxidation and consolidation defects in cup performance.* Clinical orthopaedics and related research, 1998. **352**: p. 105-117.
138. Wroblewski, B.M., *Direction and rate of socket wear in Charnley low-friction arthroplasty.* Bone & Joint Journal, 1985. **67**(5): p. 757-761.
139. Sychterz, C.J., et al., *Wear of polyethylene cups in total hip arthroplasty. A study of specimens retrieved post mortem.* J Bone Joint Surg Am, 1996. **78**(8): p. 1193-1200.

140. Jasty, M., et al., *Wear of polyethylene acetabular components in total hip arthroplasty. An analysis of one hundred and twenty-eight components retrieved at autopsy or revision operations.* J Bone Joint Surg Am, 1997. **79**(3): p. 349-58.

141. Streicher, R.M. and R. Schon, *Tribological Behavior of Various Materials and Surfaces against Polyethylene.* Trans. 17th Soc. Biomaterials, 1991. **289**.

142. Fisher, J., et al., *The effect of sliding velocity on the friction and wear of UHMWPE for use in total artificial joints.* Wear, 1994. **175**(1-2): p. 219-225.

143. Wang, A., et al., *Effect of femoral head surface roughness on the wear of ultrahigh molecular weight polyethylene acetabular cups.* Journal of Arthroplasty, 1998. **13**(6): p. 615-620.

144. Tiainen, V.-M., *Amorphous carbon as a bio-mechanical coating — mechanical properties and biological applications.* Diamond and Related Materials, 2001. **10**(2): p. 153-160.

145. Saikko, V., *A multidirectional motion pin-on-disk wear test method for prosthetic joint materials.* Journal of Biomedical Materials Research, 1998. **41**(1): p. 58-64.

146. Chanda, A., et al., *Wear and friction behaviour of UHMWPE-alumina combination for total hip replacement.* Ceramics International, 1997. **23**(5): p. 437-447.

147. Galvin, A., et al., *Penetration, creep and wear of highly crosslinked UHMWPE in a hip joint simulation* in *Society for Biomaterials 30th Annual Meeting*. 2005: Memphis, Tennessee, USA,. p. 78.

148. Saikko, V., et al., *Wear simulation of total hip prostheses with polyethylene against CoCr, alumina and diamond-like carbon.* Biomaterials, 2001. **22**(12): p. 1507-1514.

149. Saikko, V. and T. Ahlroos, *Wear simulation of UHMWPE for total hip replacement with a multidirectional motion pin-on-disk device: Effects of counterface material, contact area, and lubricant.* Journal of Biomedical Materials Research, 2000. **49**(2): p. 147-154.

150. Yao, J.Q., et al., *Effect of fluid absorption on the wear resistance of UHMWPE orthopedic bearing surfaces.* Wear, 2003. **255**(7): p. 1113-1120.

151. Saikko, V., *A Hip Wear Simulator with 100 Test Stations.* Proceedings of the Institution of Mechanical Engineers, Part H: Journal of Engineering in Medicine, 2005. **219**(5): p. 309-318.

152. Hill, M.R., et al., *Preliminary tribological evaluation of nanostructured diamond coatings against ultra-high molecular weight polyethylene.* Journal of Biomedical Materials Research Part B: Applied Biomaterials, 2008. **85B**(1): p. 140-148.

153. Saikko, V. and J. Kostamo, *Performance analysis of the RandomPOD wear test system.* Wear, 2013. **297**(1): p. 731-735.

154. Livermore, J., B. Ilstrup D Fau - Morrey, and B. Morrey, *Effect of femoral head size on wear of the polyethylene acetabular component.* (0021-9355 (Print)).

155. Cournoyer, J.R., J.A. Ochoa, and S.M. Kurtz, *Relative motion at the backside of a metal-backed acetabular component under quasistatic and dynamic loading*. 1997: Transactions of Orthopaedics Research Society.

156. Saikko, V., et al., *A Five-Station Hip Joint Simulator for Wear Rate Studies.* Proceedings of the Institution of Mechanical Engineers, Part H: Journal of Engineering in Medicine, 1992. **206**(4): p. 195-200.

157. Dowson, D., B. Jobbins, and A. Seyed-Harraf, *An evaluation of the penetration of ceramic femoral heads into polyethylene acetabular cups.* Wear, 1993. **162-164**(PART B): p. 880-889.

158. Wang, A., C. Stark, and J.H. Dumbleton, *Mechanistic and Morphological Origins of Ultra-High Molecular Weight Polyethylene Wear Debris in Total Joint Replacement Prostheses.* Proceedings of the Institution of Mechanical Engineers, Part H: Journal of Engineering in Medicine, 1996. **210**(3): p. 141-155.

159. Martinella, R., S. Giovanardi, and G. Palombarini, *Wear of ultrahigh molecular weight polyethylene sliding against surface-treated Ti6Al4V, AISI 316 stainless steel and Vitallium.* Wear, 1989. **133**(2): p. 267-279.

160. Saikko, V.O., *A three-axis hip joint simulator for wear and friction studies on total hip prostheses.* Proceedings of the Institution of Mechanical Engineers, Part H: Journal of Engineering in Medicine, 1996. **210**(3): p. 175-185.

161. Kabo, J.M., et al., *In vivo wear of polyethylene acetabular components.* The Journal of Bone and Joint Surgery. British volume, 1993. **75-B**(2): p. 254-258.

162. Sychterz, C.J., et al., *Radiographic evaluation of penetration by the femoral head into the polyethylene liner over time.* (0021-9355 (Print)).

163. Kesteris, U., et al., *Polyethylene wear in Scanhip arthroplasty with a 22 or 32 mm head: 62 matched patients followed for 7-9 years.* (0001-6470 (Print)).

164. Atkinson, J.R., et al., *Laboratory wear tests and clinical observations of the penetration of femoral heads into acetabular cups in total replacement hip joints: II: A microscopical study of the surfaces of Charnley polyethylene acetabular sockets.* Wear, 1985. **104**(3): p. 217-224.

165. Hall, R.M., et al., *Wear in Retrieved Charnley Acetabular Sockets.* Proceedings of the Institution of Mechanical Engineers, Part H: Journal of Engineering in Medicine, 1996. **210**(3): p. 197-207.

166. Paul, J.P., *Paper 8: Forces Transmitted by Joints in the Human Body.* Proceedings of the Institution of Mechanical Engineers, Conference Proceedings, 1966. **181**(10): p. 8-15.

167. Maxian, T.A., *Development and Application of A Finite Element Formulation for Estimating Sliding Wear in Total Hip Arthroplasty. PhD Thesis*. 1997, University of Iowa: Iowa City, Iowa, USA.

168. Galvin, A.L., et al., *Wear and biological activity of highly crosslinked polyethylene in the hip under low serum protein concentrations.* Proceedings of the Institution of Mechanical Engineers, Part H: Journal of Engineering in Medicine, 2007. **221**(1): p. 1-10.

169. Heller, M.O., et al., *Musculo-skeletal loading conditions at the hip during walking and stair climbing.* Journal of Biomechanics, 2001. **34**(7): p. 883-893.

170. Bigsby, R.J.A., C.S. Hardaker, and J. Fisher, *Wear of ultra-high molecular weight polyethylene acetabular cups in a physiological hip joint simulator in the anatomical position using bovine serum as a lubricant.* Proceedings of the Institution of Mechanical Engineers, Part H: Journal of Engineering in Medicine, 1997. **211**(3): p. 265-269.

171. Callaghan, J.J., et al., *Orthopaedic Crossfire®—larger femoral heads: A triumph of hope over reason!: In the affirmative.* The Journal of Arthroplasty, 2003. **18**(3, Supplement 1): p. 82-84.

172. Engh Jr, C.A., et al., *A prospective, randomized study of cross-linked and non-cross-linked polyethylene for total hip arthroplasty at 10-year follow-up.* Journal of Arthroplasty, 2012. **27**(8 SUPPL.): p. 2-7.e1.

173. Olyslaegers, C., et al., *Wear in Conventional and Highly Cross-Linked Polyethylene Cups: A 5-Year Follow-Up Study.* The Journal of Arthroplasty, 2008. **23**(4): p. 489-494.

174. Stilling, M., et al., *Clinical Comparison of Polyethylene Wear with Zirconia or Cobalt-Chromium Femoral Heads.* Clinical Orthopaedics and Related Research®, 2009. **467**(10): p. 2644-2650.

175. Ayers, D.C., et al., *Two-Year Radiostereometric Analysis Evaluation of Femoral Head Penetration in a Challenging Population of Young Total Hip Arthroplasty Patients.* The Journal of Arthroplasty, 2009. **24**(6, Supplement): p. 9-14.

176. Rajadhyaksha, A.D., et al., *Five-Year Comparative Study of Highly Cross-Linked (Crossfire) and Traditional Polyethylene.* The Journal of Arthroplasty, 2009. **24**(2): p. 161-167.

177. Huddleston, J.I., et al., *Hylamer vs Conventional Polyethylene in Primary Total Hip Arthroplasty: A Long-Term Case-Control Study of Wear Rates and Osteolysis.* The Journal of Arthroplasty, 2010. **25**(2): p. 203-207.

178.   Capello, W.N., et al., *Continued Improved Wear with an Annealed Highly Cross-linked Polyethylene.* Clinical Orthopaedics and Related Research®, 2011. **469**(3): p. 825-830.

179.   Johanson, P.-E., et al., *Highly Crosslinked Polyethylene Does Not Reduce Aseptic Loosening in Cemented THA 10-year Findings of a Randomized Study.* Clinical Orthopaedics and Related Research®, 2012. **470**(11): p. 3083-3093.

180.   Vendittoli, P.A., et al., *Alumina on alumina versus metal on conventional polyethylene: A randomized clinical trial with 9 to 15 years follow-up.* Acta Orthopaedica Belgica, 2013. **79**(2): p. 181-190.

Table 1 *In vivo* and *in vitro* wear rate of MoP (Metal-on-Polyethylene) prostheses [5, 6]

Liner Material	*In vivo* wear rate (mm/year)	*In vitro* wear rate (mm^3/million cycles)
Conventional UHMWPE	0.1	32.6
Cross-linked UHMWPE	0.01–0.2	13.6

Table 2 Wear coefficients used in numerical study of UHMWPE liner wear

Numerical Study	Bearing Material	Wear Coefficient (mm³/Nm)	Surface Roughness Effect	Cross Shear Effect	Contact Pressure Effect	Source of Wear Coefficient
Maxian et al (1996a, b, c) [21-23]	UHMWPE / CoCr	$1.0656e{-6}$	N	N	N	PoD [141] (Streicher and Schon 1991)
Maxian et al (1997) [46]	UHMWPE / SS	$1.53e{-6}$	N	N	N	Couple Simulator and FEA
Pietrabissa et al (1998) [18]	UHMWPE / CoCr	$0.235e^{-4}*Ra^{2.03}$	Y	N	N	PoD [142] (Fisher et al 1994)
Kurtz et al (1999) [50]	UHMWPE / CoCr	$1.0656e{-6}$	N	N	N	Maxian et al (1996a, b, c) [21-23]
Raimondi et al (2001) [19]	UHMWPE / CoCr	$8.686e^{-6}*Ra+1.51e^{-6}$	Y	N	N	Simulator [143] (Wang et al 1998)
Brown et al (2002) [69]	UHMWPE / CoCr	$1.0656e{-6}$	N	N	N	Maxian et al (1996a, b, c) [21-23]
Hung and Wu (2002) [86]	UHMWPE / CoCr; UHMWPE / SS; UHMWPE / Alumina	$3.5e{-7}$; $8e{-7}$; $3.1e{-7}$	N	N	N	PoD [144](Tiainen 2001); PoD [145](Saikko 1998); PoD [146] (Chanda et al 1997)
Teoh et al (2002) [54]	UHMWPE / CoCr	$1.0656e{-6}$	N	N	N	Maxian et al (1996a, b, c) [21-23]
Patil et al (2003) [88]	UHMWPE / CoCr	$1.0656e{-6}$	N	N	N	Maxian et al (1996a, b, c) [21-23]
Wu et al (2003) [87]	UHMWPE / SS	$8e{-7}$	N	N	N	PoD [145](Saikko 1998)
Bevill et al (2005) [51]	UHMWPE / CoCr	$1.0656e{-6}$	N	N	N	Maxian et al (1996a, b, c) [21-23]
Kang et al (2006) [48]	UHMWPE / CoCr	$1.0656e{-6}$; $2e{-7}$ (cross-linked)	N	N	N	Maxian et al (1996a, b, c) [21-23]; Simulator [147] (Galvin et al 2005)
Onisoru et al (2006) [79]	UHMWPE / CoCr	$7.99e^{-6}*\sigma^{-0.653}$	N	N	Y	Simulator [97] (Wang 2001)
Penmetsa et al (2006) [52]	UHMWPE / CoCr	$1.0656e{-6}$	N	N	N	Maxian et al (1996a, b, c) [21-23]
Fialho et al (2007) [57]	UHMWPE / CoCr	$1.0656e{-6}$	N	N	N	Maxian et al (1996a, b, c) [21-23]
Lundberg et al (2007) [56]	UHMWPE / CoCr	$1.0656e{-6}$	N	N	N	Maxian et al (1996a, b, c) [21-23]
Sfantos and Aliabadi (2007a) [89]	UHMWPE / SS	$8e{-7}$	N	N	N	Wu et al (2003) [87]
Sfantos and Aliabadi (2007b) [90]	UHMWPE / Alumina; UHMWPE / CoCr; UHMWPE / DLC CoCr	$1.51e{-6}$; $1.76e{-6}$; $1.80e{-6}$	N	N	N	Simulator [148] (Saikko et al 2001)
Kang et al (2008a) [67]	UHMWPE / CoCr	$3.28e^{-7}*\ln(CSR)+1.62e^{-6}$ $2e^{-8}*\ln(CSR)+2e^{-7}$(cross-linked)	N	Y	N	PoD [67] (Kang et al 2008a)
Kang et al (2009) [92]	UHMWPE / CoCr	$e^{-13.1+0.19\ln CSR-0.29\sigma}$	N	Y	Y	PoD [99] (Kang et al 2008b)
Matsoukas et al (2009) [53]	UHMWPE / CoCr	$5.322e{-7}$ (cross-linked)	N	N	N	Couple Simulator and FEA
Matsoukas and Kim (2009) [61]	UHMWPE / CoCr	$5.322e{-7}$ (cross-linked)	N	N	N	Matsoukas et al (2009) [53]
Queiroz et al (2013) [91]	UHMWPE / SS	$1e{-6}$	N	N	N	PoD [145] (Saikko 1998)
Ronda and Wojnarowski (2013) [66]	UHMWPE / CoCr; UHMWPE / SS	$3.5e{-7}$; $1.81e{-7}$	N	N	N	Hung and Wu (2002) [86]
Pakhaliuk et al (2015) [68]	UHMWPE / CoCr; UHMWPE / SS; UHMWPE / CoCr	$7.99e^{-6}*\sigma^{-0.653}$; $2e^{-6}*\sigma^{-0.84}$; $2.7e^{-6}*(\sigma/\sigma_{ref})^{-0.57}$, when $\sigma/\sigma_{ref} \leq 2.53$ $6.0e^{-6}*(\sigma/\sigma_{ref})^{-1.44}$, when $\sigma/\sigma_{ref} > 2.53$	N	N	Y	Simulator [97] (Wang 2001); PoD [101] (Vassiliou and Unsworth 2004); PoD [102] (Saikko 2006)
Lin et al (2016) [58]	UHMWPE / CoCr	$1.48e{-6}$	N	N	N	Self-average PoD [149-153]

Table 3 A summary of the input conditions, predicted wear rates from FEA studies of UHMWPE liners and model validation

FEA Study	Software Platform / Wear Modelling Code	Liner Material Property	Simulated Cycles of Wear (Mc) / year	Load & Motion	Swing Phase Included (Y/N)	Number of Steps per Load Cycle	Geometrical Update Interval due to wear (Mc)	Friction Coefficient	Liner Element Type / Count	Head Diameter (mm)	Radial Clearance (Liner Thickness) (mm)	In silico volumetric Wear Rate (mm³/Mc)	In silico linear Wear Rate (mm/Mc)	In vivo/vitro volumetric Wear Rate (mm³/Mc)	In vivo/vitro linear Wear Rate (mm/Mc)	Further Details
Maxian et al (1996b) [22]	ABAQUS v5.3 + FORTRAN	UHMPWE: E=1400 MPa	1	3D loading + 1D angular motion [134]	N	16	~	0	6-node wedge + 8-node brick /1080 elements (4 layers)	22	~	13	0.110	0 - 146	0.13 ± 0.10	Indirect validation against *in vivo* data [154]
										28	~	16	0.111	0 - 225	0.08 ± 0.07	
										32	~	18	0.116	3 - 256	0.10 ± 0.06	
Maxian et al (1996c) [23]	ABAQUS v5.3 + FORTRAN	UHMPWE: E=1400 MPa	20	3D loading + 1D angular motion [134]	N	16	0.5	0	6-node wedge + 8-node brick /3864 elements (3 layers)	22	~(11)	14.3	0.0433	~		Adaptive meshing technique
										22	~(6)	14.4	0.0438			
										22	~(3)	14.5	0.0441			
										28	~(8)	17.9	0.0366			
										32	~(6)	20.4	0.0319			
Kurtz et al (1999) [50]	LS-DYNA3D + C	UHMPWE(GUR 415): E=974MPa, *V*=0.46; Plastic strain: 0, 0.011, 0.0367, 0.0914, Yield Stress (MPa): 14.0, 22.1, 27.1, 29.5.	1	1D loading + 1D angular motion [155]	Y	14	~	0.083	8-node brick / ~ elements (1 layer)	28	0.1(7.8)	38.6-39.0	0.212-0.229	16	0.111	Wear results of models without screw holes. Indirect validation against *in silico* data[22]
Brown et al (2002) [69]	ABAQUS v5.3 + FORTRAN	UHMPWE: ~	1	3D loading + 1D angular motion [134]	N	16	0.04 (15 days)	~	6-node wedge + 8-node brick /1800 elements (3 layers)	28	0.25(8)	19.8	0.08	~		Wear results of models without head roughening
Hung & Wu (2002) [86]	FORTRAN	UHMPWE: E=800MPa, *V*=0.47	1.5 (1 year)	1D loading + 1D angular motion	Y	16	0.1	~	8-node brick / 1044 elements (3 layers)	22	~(28)	18.2	0.048	~		UHMWPE / CoCr. Indirect validation
										28	~(22)	23.0	0.037	~	0.247 (*in vivo* [157]);	

Study	Software	Material	Time	Loading		FE			Mesh	Diameter				Validation		Notes
				[145, 156]										0.091 (*in vitro* [148])		
														0.053 (*in vitro* [158])		
										32	~(18)	29.13	0.036	~	0.022 (*in vitro* [159])	
														0.003 (*in vitro* [160])		
Teoh et al (2002) [54]	ABAQUS v5.7	UHMP WE: E=1400 MPa, *V*=0.3	~	3D loading + 1D angular motion [134]	N	16	~	0 – 0.3	8-node brick / 1500 elements (4 layers)	32	0.001	122.27	0.23	~		Perfect plasticity material model. Indirect validation.
											0.05	56.69	0.11			
											0.1	53.68	0.1			
											0.15	56.33	0.1			
											0.2	56.89	0.12	18 (*in silico* [22])	0.116 (*in silico* [22])	
														90 ± 44 (in vivo [154, 161-163])		
											0.3	63.10	0.22	~		
											0.5	114.72	0.31	~		
Wu et al (2003) [87]	FORTRAN	UHMP WE: E=800MPa, *V*=0.47	1.5 (1 year)	1D loading + 1D angular motion [145, 156]	Y	16	0.1	~	8-node brick / 1044 elements (3 layers)	22	0(28)	42.04	0.111	1.9 – 237 (mean: 74) [164]	0.005 – 0.623 (mean: 0.19) [164]	Indirect validation with *in vivo* [154, 164, 165] and *in silico* [22] studies
														0 – 147 (mean: 47.5) [154]	0 – 0.39 (mean: 0.13) [154]	
														~	0.1 – 0.15 [165]	
														55 [165]	0.2 [165]	
														13 [22]	0.11 [22]	
										24	~	45.639	0.101	~		
										26	~	48.901	0.092			
										28	~	52.072	0.085	0 – 225 (mean:48.4) [154]	0 – 0.3 (mean: 0.08) [154]	
														16 [22]	0.111 [22]	
										30	~	55.224	0.078	~		
										32	~	58.417	0.073	3 – 256 [154]	0 – 0.32 [154]	
														18 [22]	0.116 [22]	
Bevill et al (2005) [51]	ABAQUS v6.3 + Python	UHMP WE: E=1400 MPa, *V*=0.3	1	3D loading + 1D angular motion [134]	N	16	0.5	~	8-node brick / 6800-15500 elements	22	0.2 (4-16)	12*	0.07*	In-direct validation: 4.4% increase in volumetric wear per mm increase of head dimeter (this study) vs. 4.3% (*in silico* [21]) & 5% (*in vitro* [21])		*Estimated mean value of different liner thickness
										28	0.2 (4-16)	15*	0.07*			
										32	0.01-0.5	19.1-16.2	0.03-0.08			
										36	0.2 (4-16)	19.5*	0.07*			
Kang et al (2006) [48]	~	Cross-linked UHMP WE:	20	3D loading + 3D angular motion	Y	21	0.125	~	6-node wedge + 8-node brick / mesh	28	0.2	85.2*	0.24*	~		*Cumulated wear results over 20 years
										32		96.4*	0.22*			
										34		101.98*	0.21*			
										38		113*	0.2*			
										42		124*	0.18*			

Study	Software	Material		Loading + motion			Time step		Element							Description
		E=1400 MPa, V=0.3		[135, 166]					grid = 30*30	46		134.9*	0.17*			
										48		140.3*	0.17*			
		Conventional UHMPWE: E=1000 MPa, V=0.4								28	0.001 (8)	28.3	0.048	~		Wear results of various clearance
											0.1 (8)	28.3	0.047			
											0.3 (8)	28	0.046			
											0.5 (8)	27.6	0.045			
											1 (8)	26.7	0.044			
										18	~	18.1	0.065	15.6	0.067	Average wear rates over 20 years. Indirect validation (in silico [167])
										22.225		22.4	0.056	19.1	0.056	
										26		26.2	0.05	22.2	0.049	
										28		26.5	0.044	23.9	0.046	
										32		32.3	0.042	27.1	0.041	
										34		34.3	0.040	28.6	0.04	
Lundberg et al (2007) [56]	~	~	1	3D loading + 1D angular motion [134] (walking)	N	16	0.041667 (2 weeks)	~	8-node brick / ~ elements	~	~	22.30	0.1	~		Wear results from head roughening not listed
				3D loading + 3D angular motion [63] (stair ascending)								22.21	0.1			
Fialho et al (2007) [57]	ANSYS	UHMPWE: E=2200 MPa, V=0.3	1	3D loading + 3D angular motion [63]	N	28	~	0.07	8-node brick / ~ elements	28	0.001	18	0.09	16 (in silico [22])	0.11 (in silico [22])	Patient: KWR Indirect validation
														0 - 225 (in vivo [154])	0.08 ± 0.07 (in vivo [154])	
												25.6	0.12	~		Patient: HSR
												40	0.21			Patient: EBL (jogging)
Kang et al (2008a) [67]	MATLAB 7.0 + Fortran 95	~	5	1D loading [166]+ 3D angular motion [135]	Y	~	0.125	~	~ / mesh grid = 60*60	28	~	26.7	0.07	Indirect validation: 1 – 225, mean=48.4 (in vivo [154])	Indirect validation: 0 - 03 mean=0.08 (in vivo [154])	Cross shear dependent
												24.7	0.06			Cross shear independent

Study	Software	Material		Loading	Y/N				Element							Notes
Matsoukas and Kim (2009) [61]	ANSYS + Matlab	UHMPWE: $\sigma = 20.29(1 - e^{-32.485\varepsilon})$ ($\sigma < 17MPa$) E=110MPa ($\sigma > 17MPa$) 39	1	3D loading + 3D angular motion [63]	Y	21	0.25	0.08	8-node brick / ~ elements	31	0.255	16.15	0.025	17.14 ± 1.23 (sample 1); 19.39 ± 0.79 (sample 2) [53]	Total damage (3Mc)=0.329 (in silico) vs. 0.337 (sample 1, 0.116 of wear & 0.2221 of creep)[53]	Walking. Direct validation by the same group [53].
												24.0	0.034	~		Stair ascending
Kang et al (2009) [92]	~	~	5	1D loading + 2D motion [65]	Y	~	~	~	~	28	0.2(22)	14	0.082*	38 ± 1.1	0.25 ± 0.004	*Max. penetration at 2Mc. Direct validation (in vivo)
Barreto et al (2010) [47]	ABAQUS v6.7	UHMPWE: E=1400 MPa, V=0.46	1	3D loading+ 3D angular motions [57, 63]	N	28	1	0.07	8-node brick / ~ elements	28	0.001 (14)	17.76-18.13	0.067-0.085	~		Wear results with (without) metal shell & Pelvic bone
										32	0.001 (12)	17.62-18.11	0.051-0.074			
Liu et al (2010) [49]	ABAQUS v6.8-1	UHMPWE (GUR 1050): E=500MPa, V=0.4; Plasticity [95]	10	1D loading + 2D motion [65]	Y	~	0.25	~	8-node brick / 2000 elements (0.5mm)	28	0.2 (8)	23	0.042	39 (in vivo) / 14 (in silico [92])	~	Direct validation with studies of the same group
Liu et al (2012) [65]	ABAQUS v6.8-1	UHMPWE (GUR 1050): E=500MPa, V=0.4; Plasticity [95]	5	1D loading + 2D motion [65]	Y	~	0.25	~	8-node brick / 2000 elements (0.5mm)	22	0.02-0.35	4.0-6.0	~	~		Wear rate at clearance ranging 0.02 – 0.35 mm. Direct validation with studies of the same group
										28	0.02-0.35	6.0-13.7	~	Accumulated volume change = 40mm³ (this study) vs. 25 mm³ (in vitro) [168]	Total damage=0.1mm (this study) vs. 0.05 mm (in vitro) [168]	
										36	0.02-0.35	10.0-24.0	~	~		
Ronda and Wojnarowski (2012) [66]	ABAQUS	UHMPWE: E=1240 MPa, V=0.4; Plasticity [66]	10	3D loading + 3D angular motion [169]	Y	~	~	~	8-node brick / ~ elements	22	0(24)	27.28-31.19	0.072-0.082	~	~	UHMWPE / CoCr wear results of various inclination and anteversion angles. Indirect validation
										28	0(18)	27.55-30.60	0.045-0.049	~	0.037 (in silico [86]) / 0.091 (in vitro [148])	
										32	0(14)	22.59-30.55	0.033-0.038	~	0.036 (in silico [86])	

| Study	Software	Material		Loading / motion					Mesh / elements							Notes
															0.053 (*in vitro* [158])	
Liu et al (2013) [60]	ABAQUS v6.8-1	UHMPWE (GUR 1050): E=500MPa, *V*=0.4; Plasticity [95]	5	3D loading + 3D motion (Measured gait) [135]	Y	~	0.25	~	8-node brick / 2000 elements (0.5mm)	28	0.04 (8)	14.0	~	38 (*in silico* [95])	~	Indirect validation
				1D loading + 3D motion (ISO14242-1) [64]								13.4	~	~	~	
				1D loading + 2D motion (Leeds ProSim Hip Simulator) [65]								12.2	~	32 (*in vitro* [170])	~	
Queiroz et al (2013) [91]	ANSYS v12.0	UHMPWE: E=1400 MPa, *V*=0.35	1	3D loading + 1D angular motion [134]	N	16	~	~	10 node tet (SOLID92)/ ~ elements	28	0.1 (10)	30.85	0.19	~		Inclination: 30°
												30.97	0.17	48.4 [154]	0.08 [154]	Inclination: 45°. Indirect validation (*in vivo*)
														34 [171]	0.09 [171]	
												47.41	0.26	~		Inclination: 60°
Pakhaliuk et al (2015) [68]	ANSYS + Matlab	UHMPWE: E=1400 MPa, *V*=0.46	3	1D loading + 3D motion (ISO14242-1)[64]	Y	25	0.125—0.25	~	~ / mesh grid = 30*30	32	0.15(8)	18.5-21.8	0.046-0.079	~		Various wear coefficient used
Lin et al (2016) [58]	~	UHMPWE: E=800MPa, *V*=0.47	7.5 (5 years)	1D loading + 1D angular motion [145, 156]	Y	16	0.75	0	8-node brick / ~ elements	28	0	58.16	0.169	Indirect validation (*in vivo*): 119 [172]	Indirect validation (*in vivo*): 0.22 [172]; 0.101 [173]; 0.25 [174]; 0.085 [175]; 0.127 [176]; 0.2 [177]; 0.14 [178]; 0.055 [179]; 0.19 [180]	One service year
												60.21	0.181			Ten service years
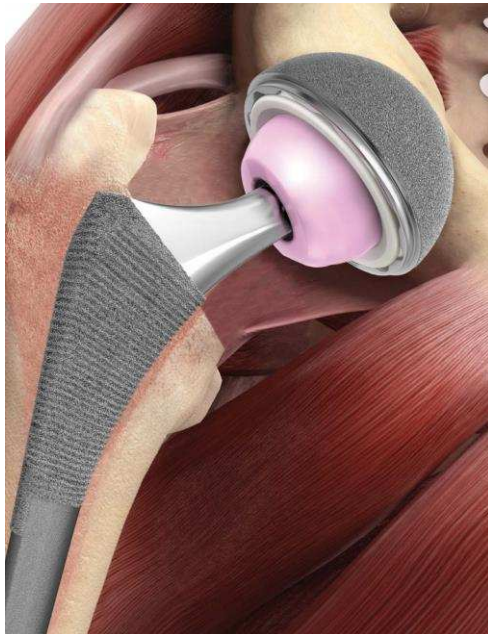
Figure 1 Polyethylene total hip joint. Image courtesy of DePuy Synthes, Leeds, UK

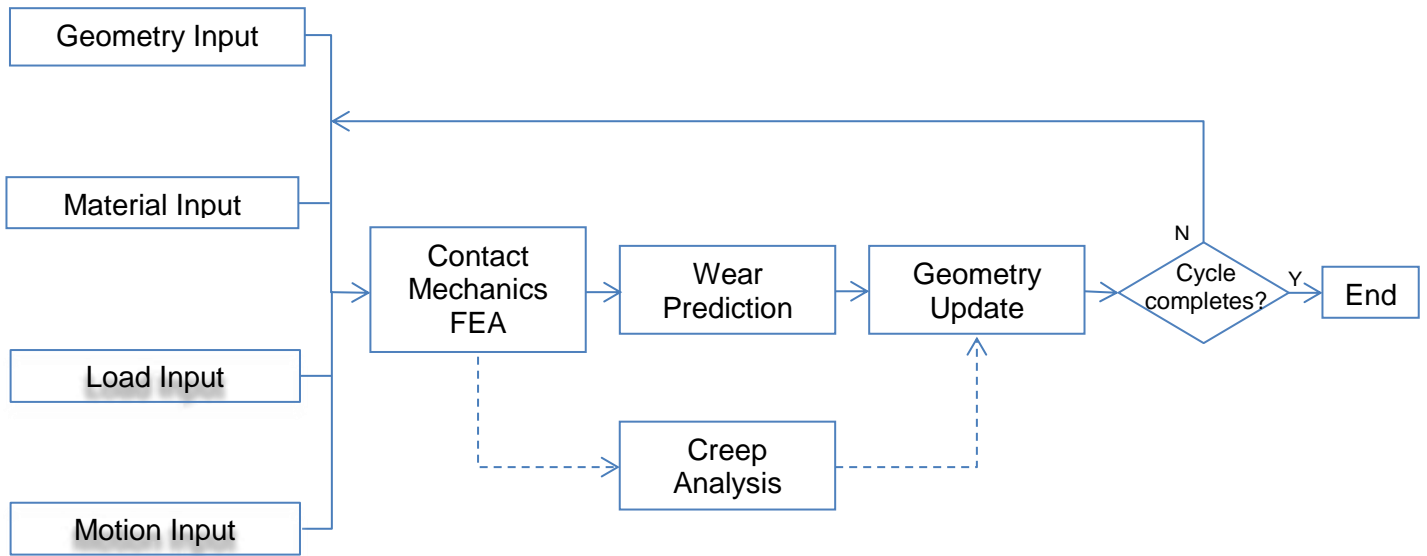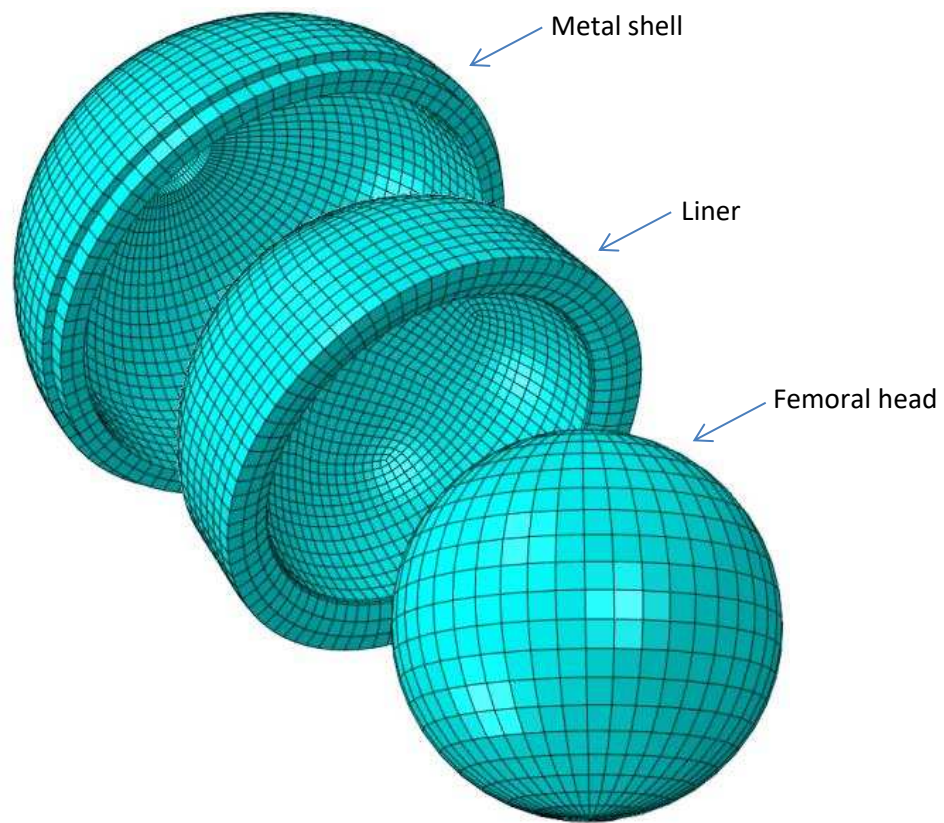Figure 2 Workflow of FEA modelling of liner wear

Figure 3 An exploded view of the three components commonly modelled in FEA of UHMWPE liner wear
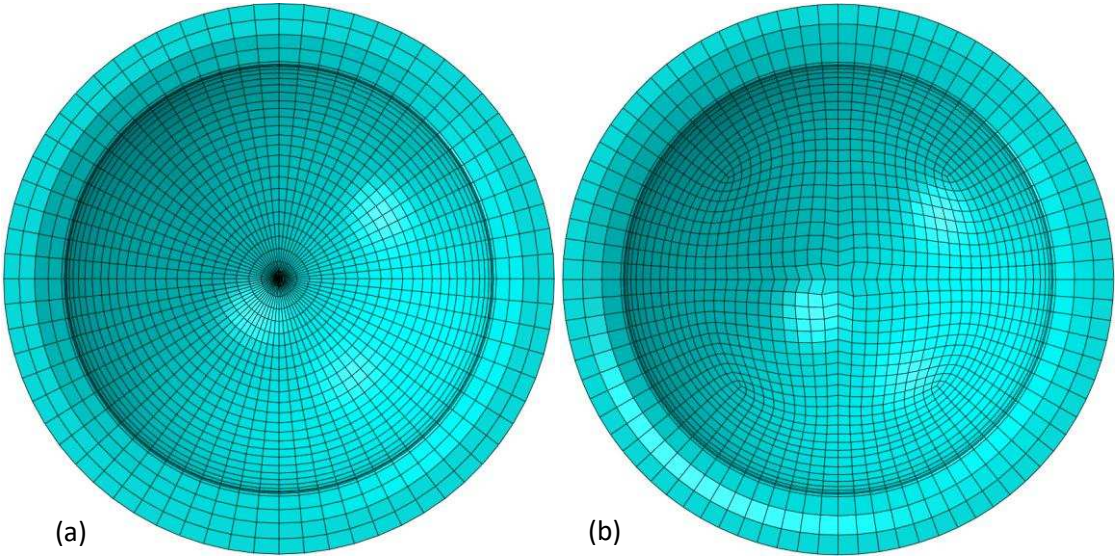
(a)　　　　　　　　　　　　　　　　　　(b)

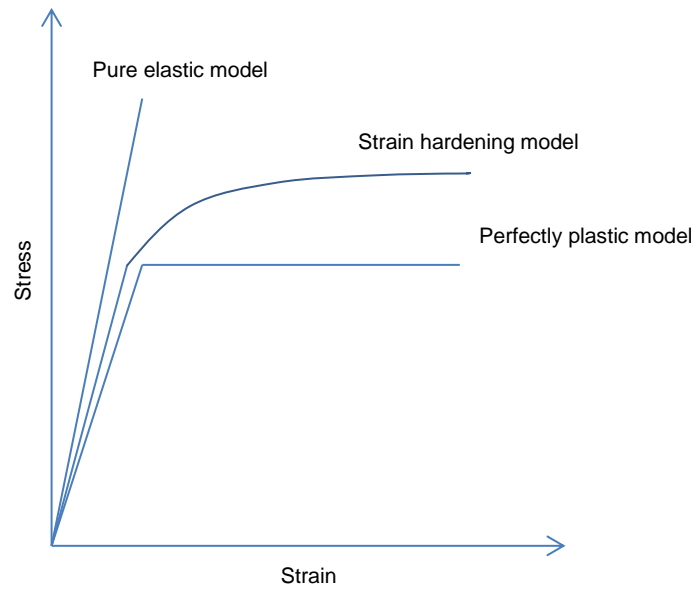Figure 4 Two commonly used liner mesh configurations: (a) "polar" design, (b) "butterfly" design.

Figure 5 Schematic stress-strain behaviour exhibited by different material models used to represent the UHMWPE liner
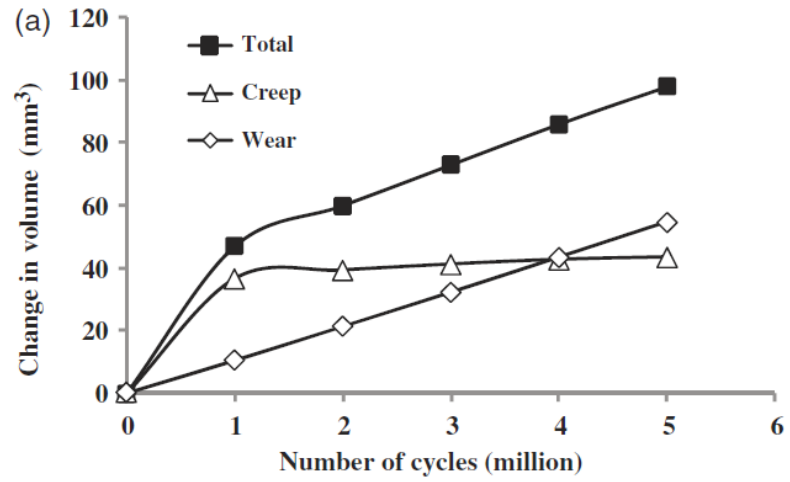
Figure 6 FEA prediction of creep, wear and total volume change. Reprinted from Liu et al [65], with permission from SAGE Publishing
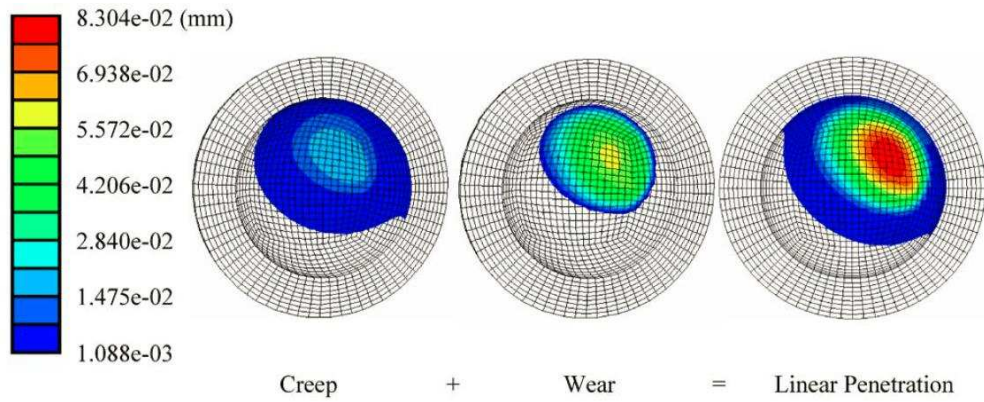
Figure 7 Contour plots showing the magnitude of creep, wear and total penetration after 1 million cycle, predicted using FEA. Reprinted from Bevill et al [51], with permission from Elsevier